# Bystander memory-phenotype conventional CD4$^+$ T cells exacerbating autoimmune neuroinflammation

Min-Zi Cho[1,†], Hong-Gyun Lee[1,2,†], Jae-Won Yoon[1], Gil-Ran Kim[1], Ja-Hyun Koo[1,3], Reshma Taneja[4], Brian T. Edelson[5], You Jeong Lee[6], Je-Min Choi[1,7,8,*]

[1]Department of Life Science, College of Natural Sciences, Hanyang University, Seoul 04763, Republic of Korea.
[2]Ann Romney Center for Neurologic Diseases, Brigham and Women's Hospital, Harvard Medical School, Boston, MA 02115, USA.
[3]The Ragon Institute of Massachusetts General Hospital, Massachusetts Institute of Technology and Harvard University, Cambridge, MA 02139, USA.
[4]Department of Physiology and Healthy Longevity Translation Research Program, Yong Loo Lin School of Medicine, National University of Singapore, Singapore 117593.
[5]Department of Pathology and Immunology, Division of Laboratory and Genomic Medicine, Washington University School of Medicine, St. Louis, MO 63119, USA.
[6]Research Institute of Pharmaceutical Sciences, Seoul National University, Seoul, Republic of Korea.
[7]Research Institute for Natural Sciences, Hanyang University, Seoul 04763, Republic of Korea.
[8]Research Institute for Convergence of Basic Sciences, Hanyang University, Seoul 04763, Republic of Korea.

†These authors contributed equally to this work.
[*]Corresponding author. Email: jeminchoi@hanyang.ac.kr

Keywords: Memory-phenotype CD4$^+$ T cells, Bystander, EAE, Autoimmune neuroinflammation, CCR6, TCR independent, Bhlhe40

## Abstract

Memory-phenotype (MP) $CD4^+$ T cells are a substantial population of conventional T cells that exist in steady-state mice, and their immunologic functions in autoimmune disease have not yet been studied. In this work, we unveil a unique phenotype of MP $CD4^+$ T cells by analyzing single-cell transcriptomics and T cell receptor (TCR) repertoires. We found that steady-state MP $CD4^+$ T cells exist regardless of germ and food-antigen which are composed of heterogenous effector subpopulations. Distinct subpopulations of MP $CD4^+$ T cells are specifically activated by IL-1 family cytokines and STAT activators, revealing that the cells have TCR-independent effector functions. Especially, $CCR6^{high}$ MP $CD4^+$ T cells are major responders to IL-1β and IL-23 without $MOG_{35-55}$ antigen reactivity, which gives them pathogenic-Th17 characteristics and allows them to contribute to autoimmune encephalomyelitis. We identified Bhlhe40 in $CCR6^{high}$ MP $CD4^+$ T cells drives the expression of GM-CSF, contributing to CNS pathology in experimental autoimmune encephalomyelitis. Collectively, our findings reveal heterogeneity of MP $CD4^+$ T cells that can contribute to autoimmune neuroinflammation in bystander manner synergistically with antigen-specific T cells.

43 **Introduction**

44 The immunological memory of antigen-specific T cells enables faster and more potent responses upon re-
45 exposure to a previously encountered antigen, providing long-lasting immunity (Kaech & Cui, 2012). Although
46 a substantial population of memory-phenotype (MP) conventional T cells exists in steady state mice unexposed
47 to foreign antigens, it has been reported that MP T cells are formed before birth in humans and exist in germ-
48 free (GF) and antigen-free (AF) conditioned mice (Byrne *et al*, 1994; Dobber *et al*, 1992; Haluszczak *et al*,
49 2009; Szabolcs *et al*, 2003).

50 After undergoing homeostatic proliferation in a lymphopenic environment, naïve T cells acquire
51 phenotypical, functional, and gene expression–like antigen-specific memory and become MP T cells (Cho *et al*,
52 2000; Ernst *et al*, 1999; Goldrath & Bevan, 1999; Goldrath *et al*, 2004). T cell receptor (TCR) and CD28
53 signaling seem to be required for the conversion of naïve $CD4^+$ T cells into MP T cells. MP $CD4^+$ T cells express
54 CD5, a marker with high affinity to self-antigen, and resist infection by mediating a Th1-like immune response
55 without antigen stimulation (Kawabe *et al*, 2017). A previous study confirmed that antigen-non-specific MP
56 $CD4^+$ T cells proliferated more than Lymphocytic choriomeningitis virus (LCMV)-specific T cells in an LCMV
57 infection model. Indeed, treatment with an anti-MHCII antibody did not inhibit the proliferation of MP $CD4^+$ T
58 cells, suggesting that they play a bystander role against infection (Younes *et al*, 2011).

59 Unlike MP $CD4^+$ T cells, MP $CD8^+$ T cells have been well studied for their antigen-specific and
60 bystander functions. MP $CD8^+$ T cells can rapidly produce IFN-γ upon stimulation with IL-12 and IL-18 and
61 without cognate antigen stimulation (Sosinowski *et al*, 2013; White *et al*, 2017). In particular, MP $CD8^+$ T cells
62 are called virtual memory. They can have specific reactions to certain antigens without previous exposure (Akue
63 *et al*, 2012; Haluszczak *et al.*, 2009; Hamilton *et al*, 2006; Sosinowski *et al.*, 2013; White *et al*, 2016) and
64 increase NKG2D and granzyme B expression upon IL-12, IL-18, and IL-15 stimulation, producing a bystander
65 killing role against infection (Chu *et al*, 2013; Lertmemongkolchai *et al*, 2001; White *et al.*, 2016). In addition,
66 MP $CD8^+$ T cells can play an antigen-specific protection role in *Listeria monocytogenes*, Herpes simplex virus
67 (HSV), and *vaccinia* infections (Haluszczak *et al.*, 2009; Hamilton *et al.*, 2006; Lee *et al*, 2013a; Sosinowski *et*
68 *al.*, 2013). Also, MP $CD8^+$ T cells have high affinity to self-antigens, so they can break peripheral tolerance
69 with MP $CD4^+$ T cells and develop autoimmune diabetes (King *et al*, 2004; Le Saout *et al*, 2008). Overall,
70 previous studies have shown the function of MP $CD8^+$ T cells in disease, but the role of MP $CD4^+$ T cells in
71 autoimmune disease has not yet been studied.

72 Most previous studies have focused on the role of autoantigen-specific T cells in both humans and
73 mice to understand autoimmune diseases and find therapeutic drugs to regulate antigen-specific T cells (Serra
74 & Santamaria, 2019). Interestingly, antigen-non-specific T cells, including myelin oligodendrocyte glycoprotein
75 (MOG) tetramer–negative $CD4^+$ Th17 cells, also infiltrate the Central nervous system (CNS) in significant
76 proportions and exacerbate experimental autoimmune encephalomyelitis (EAE) pathogenesis (Jones *et al*, 2003;
77 Lee *et al*, 2019; Lees *et al*, 2010; Lin *et al*, 2016). In support, myelin-specific T cells were found to be similar
78 in Multiple sclerosis (MS) patients and healthy controls (Hellings *et al*, 2001; Hemmer *et al*, 1997). Bystander-

activated T cells and Epstein-Barr virus–specific $CD8^+$ T cells are clonally expanded and correlate with disease pathogenesis in the joints of chronic inflammatory arthritis and Sjogren's syndrome patients (Brennan *et al*, 2008; Kobayashi *et al*, 2004; Tan *et al*, 2000), raising questions about the role of antigen-nonrelated T cells in autoimmune disease.

In this study, we hypothesized that MP conventional $CD4^+$ T cells could be encephalitogenic bystander cells during the development of autoimmune neuroinflammatory disease. First, we examined the heterogeneity of MP $CD4^+$ T cells using single cell RNA-sequencing (scRNA-seq) and TCR sequencing analyses. We found distinct subpopulations of Th1-, Th17-, Treg-, and Tfh-like cells among MP $CD4^+$ T cells. Those cells respond to IL-1 family cytokines and STAT activators, even without TCR stimulation. We further found that $CCR6^{high}$ MP $CD4^+$ T cells are the major responders to IL-1β and IL-23, expressing pathogenic signature genes in a bystander manner and thereby contributing to the development of MOG antigen–specific T cell–derived EAE. In this context, Bhlhe40 regulates the production of GM-CSF in $CCR6^{high}$ MP $CD4^+$ T cells, exacerbating EAE pathogenesis. Our findings indicate the pathogenic role of antigen-unrelated MP conventional $CD4^+$ T cells along with antigen-specific T cells during autoimmune neuroinflammatory disease.

## Results

### Single cell RNA-sequencing identifies distinct effector-like phenotypes in steady-state MP conventional $CD4^+$ T cells.

Steady-state, unprimed specific-pathogen-free (SPF)-housed mice have a significant proportion of MP $CD4^+$ T cells ($TCR\beta^+CD1d$ $tetramer^-CD8^-CD4^+CD25\text{-}CD44^{high}CD62L^{low}$) in their spleen, thymus, inguinal lymph nodes (iLNs), mesenteric lymph nodes (mLNs), Peyer's patches (PPs), and lung tissues (Fig. S1A and Fig. 1A). The proportion and number of $CD4^+$ T cells increased with age in all tissues (Fig. S1). To identify and focus on the characteristics of MP $CD4^+$ T cells, we used fluorescence-activated cell sorting (FACS) to sort MP $CD4^+$ T cells from the spleens of 10-week-old C57BL/6 mice and performed scRNA-seq with paired V(D)J sequencing of the T cell receptor (Fig. S2A to D). Also, we generated a pipeline to filter out PLZF and TCR $V_\alpha14\text{-}J_\alpha18$ (TRAV11-TRAJ18) expressing cells, a well-known key transcription factor for the development of NKT and MAIT cells (Koay *et al*, 2016; Kovalovsky *et al*, 2008; Savage *et al*, 2008). An unbiased clustering analysis revealed clearly distinct effector T cell–like subpopulations (Fig. 1B) and differentially expressed genes (DEGs) defining each cluster (Fig. 1C and D). A Gene Ontology (GO)/Kyoto Encyclopedia of Genes and Genomes (KEGG) analysis of each cluster indicated that clusters 3 and 5 were Th1- and Th17-like populations, respectively, with significance in "chemokine-mediated signaling pathway" and "cellular response to interleukin-1" (Fig. S3). In addition, lineage-specific transcription factors and chemokine receptors were localized in each cluster (Fig. 1E and Fig. S4), suggesting that MP $CD4^+$ T cells are composed of Th1-, Th17-, Tfh-, and Treg-like populations. To examine whether the subpopulations of steady-state MP $CD4^+$ T cells depended on germ or food antigens, we analyzed the proportion of $CD44^{high}CD62L^{low}$ MP $CD4^+$ T cells in the tissues of SPF-, GF-, and AF-housed mice using flow cytometry. The proportions of total MP $CD4^+$ T cells were almost identical in the spleen and other tissues except the mLN and PP (Fig. 1F, Fig. S5A and S5B),

115 indicating that the generation of splenic MP CD4$^+$ T cells is not affected by the microbiome or food antigen
116 stimulation. Our scRNA-seq analysis further confirmed that the SPF- and GF-housed mice had identical
117 proportions of distinct subpopulations of splenic MP CD4$^+$ T cells (Fig. 1G and 1H), but the proportion of Th17-
118 like MP cells in the mLNs of GF-housed mice was much lower than that in the mLNs of SPF-housed mice (Fig.
119 1I and 1J). In support, the proportion of CCR6$^{high}$ or RORγt$^+$ MP CD4$^+$ T cells in the mLNs of GF-housed mice
120 was lower than that in SPF-housed mice, suggesting that the generation of gut MP CD4$^+$ T cells is specifically
121 dependent on germs (Fig. S6). The TCR clonal diversity of MP CD4$^+$ T cells in GF-housed mice, especially the
122 Th17-like population in the mLNs, was reduced compared with SPF-housed mice, though comparable diversity
123 was observed in the spleen (Fig. 1K and 1L). Together, these data indicate that steady-state splenic MP CD4$^+$ T
124 cells contain heterogeneous subpopulations of Th1-, Th17-, Tfh-, and Treg-like cells that express effector
125 molecules and exist independently of the gut microbiome and food antigens.

126 **Phenotypic differences of MP CD4$^+$ T cells after exposure to IL-1 family and STAT activating cytokines.**

127 To determine the effector functions of MP CD4$^+$ T cells to respond to various cytokines, we performed scRNA-
128 seq of MP CD4$^+$ T cells cultured in conditioned medium with IL-12/IL-18, IL-25/IL-33, and IL-1β/IL-23
129 cytokines (Fig. 2A and Fig. S2E). Additionally, IL-7 was added to the culture medium for T-cell survival and
130 maintenance (Kondrack *et al*, 2003). The merged Uniform Manifold Approximation and Projection (UMAP)
131 plot shows phenotypic characteristics of Th1-, Th2-, Th17-, and Treg-like subpopulations (Fig. 2B and C),
132 which express lineage specific genes (Fig. 2D). Each cytokine set induced distinct subpopulations localized
133 exclusively in the plot (Fig. 2E). We further confirmed the expression of selected gene sets related to the Th1,
134 Th2, and Th17 lineages in each bystander-activated condition, which shows that type 1, 2, and 3 cytokines can
135 upregulate lineage-specific genes in MP CD4$^+$ T cells (Fig. 2F and G). A single-cell regulatory network
136 inference and clustering (SCENIC) analysis in each cytokine condition revealed a significant level of common
137 or specific transcription factor activity (Fig. 2H). In addition, an Ingenuity pathway analysis (IPA) showed the
138 predicted transcriptional regulators in each condition and speculated that the target transcription factors included
139 Bhlhe40, which can be a potent regulator of bystander activation in MP CD4$^+$ T cells (Fig. 2I). To evaluate the
140 effector functions of MP CD4$^+$ T cells, we treated MP CD4$^+$ T cells with those cytokines and/or anti-CD3/anti-
141 CD28 (Fig. 2J and 2K). Consistently, the MP CD4$^+$ T cells responded to IL-12/IL-18, IL-25/IL-33, and IL-
142 1β/IL-23 cytokines without TCR stimulation, and T-bet$^+$ IFN-γ$^+$, GATA3$^+$IL-13$^+$, and RORγt$^+$IL-17$^+$ cells
143 increased compared to TCR-stimulated condition (Fig. 2J). However, TNF-α was produced only in the presence
144 of TCR stimulation and IFN-γ in the culture supernatant from IL-12/IL-18-conditioned MP CD4$^+$ T cells, and
145 IL-4 was also significantly detected with TCR stimulation but not in the bystander condition with IL-25/IL-33.
146 Similarly, Granulocyte-macrophage colony-stimulating factor (GM-CSF) was secreted more efficiently with
147 IL-1β/IL-23 and TCR stimulation than with the cytokines alone (Fig. 2K). Collectively, these results indicate
148 that MP CD4$^+$ T cells have functional heterogeneity when responding to specific sets of IL-1 family and STAT
149 activators in the absence of their cognate antigen and suggest possible potent transcriptional regulators that
150 control MP CD4$^+$ T cell effector functions.

151 **Potential responder MP CD4$^+$ T cells express distinct chemokine receptors upon IL-12/IL-18 and IL-**
152 **1β/IL-23 stimulation.**

153 To determine which MP CD4$^+$ T cells are potential responders to IL-1 family and STAT activating cytokines,
154 we analyzed the subpopulation of expanding or responding clusters and performed trajectory analyses. Control
155 MP CD4$^+$ T cells cultured with IL-7 produced a significantly separate population of CXCR3$^{high}$ cells. In IL-
156 18/IL-12-conditioned MP CD4$^+$ T cells the CXCR3$^{high}$ cell population was reduced, and the IFN-γ- or IL-
157 13$^{high}$expressing Th1 and proliferating Th1 populations were greatly increased (Fig. 3A and 3B). Th1 signature
158 genes, *Tbx21, Ifng, Cxcr3, Il2rb1, Il18r1*, and *CCR5* were highly expressed by IL-18/IL-12-conditioned MP
159 CD4$^+$ T cells (Fig. 3C). GO/KEGG analysis indicated that the related gene sets in those cells had increased
160 including "Cellular response to interferon-gamma", "Cytokine cytokine receptor interaction", "Alzheimer's
161 disease", and "Parkinson's disease" (Fig. 3D). The IPA returned terminologies related to cytokines and
162 inflammation such as "JAK/STAT signaling" and "neuroinflammation signaling pathway" and related to
163 cytotoxic response including "Granzyme B signaling" (Fig. 3E). In a pseudo-time trajectory analysis, the MP
164 CD4$^+$ T cells formed a continuous progression that started in CXCR3$^{high}$ cells and gradually progressed toward
165 Fate 1, which expressed *Ifng, Stat5a, Bhlhe40, Batf3, Irf4* and *Irf8* (Fig. 3F and 3G). Similarly, a CCR6$^{high}$
166 cluster was present in IL-7-conditioned MP CD4$^+$ T cells, and its Th17-like cluster was specifically increased
167 by IL-1β and IL-23 (Fig. 3H and 3I). Th17 signature genes, *Rorc, Ccr6, Il17a Il1r1, Il23r*, and proliferating
168 marker *Mki67* were expressed by those cells (Fig. 3J). GO/KEGG analysis predicted that the related gene sets
169 in IL-1β /IL-23-cultured MP CD4$^+$ T cells had increased "Alzheimer's disease," "Parkinson's disease," and
170 "Huntington's disease" which are neurological diseases and also increased "cytokine signaling pathway" (Fig.
171 3K). The IPA more clearly explained the related pathways, "STAT3 pathway," "leukocyte extravasation
172 signaling," "neuroinflammation signaling pathway," "chemokine signaling," and "Th17 activation pathway"
173 (Fig. 3L). In the trajectory analysis, CCR6$^{high}$ cells seemed to be the starting point, and then the cells gradually
174 differentiated toward Fate 2 (Fig. 3M), which expresses pathogenic Th17-related genes such as *Rorc, Il17a,*
175 *Csf2, Il22, Bhlhe40, Rora and Cebpb* with increased activities (Fig. 3N) and expression level (Fig. 3O) of related
176 transcriptomes. These results collectively reveal that Th1-like and Th17-like MP CD4$^+$ T cells expressing
177 different chemokine receptors respond specifically to IL-12/IL-18 and IL-1β/IL-23 cytokines with the effector
178 functions.

179 **CCR6$^{high}$ memory phenotype CD4$^+$ T cells are bystander-activated by IL-1β and IL-23 to become**
180 **pathogenic Th17-like cells.**

181 Since scRNA-seq predicted that CCR6$^{high}$ cells were the major cells responding to IL-1β and IL-23, we sorted
182 splenic CCR6$^{high}$ and CCR6$^{low}$ MP CD4$^+$ T cells (Fig. 4A and 4B) and then determined their proportions in
183 steady-state SPF- and GF-housed mice (Fig. 4C). We found that splenic CCR6$^{high}$ MP CD4$^+$ T cells were
184 independent of the gut (Fig. 4C). CCR6$^{high}$ MP CD4$^+$ T cells expressed RORγt more highly than CCR6$^{low}$ cells
185 and had comparable expression of T-bet (Fig. 4D and 4E). Steady-state CCR6$^{high}$ MP CD4$^+$ T cells, but not
186 CCR6$^{low}$, expressed IL-17A (Fig. 4F and 4G), suggesting that CCR6$^{high}$ MP CD4$^+$ T cells are Th17-like cells.
187 Further stimulation by IL-1β and IL-23 induced IL-17A and GM-CSF expression (Fig. 4H and 4I), which

188 confirms that CCR6$^{high}$ MP CD4$^{+}$ T cells produce pathogenic cytokines in the bystander manner. The amount
189 of cytokine secreted, as determined by ELISA, consistently showed that CCR6$^{high}$ MP CD4$^{+}$ T cells, but not
190 CCR6$^{low}$, significantly produced IL-17A, GM-CSF, and IFN-γ and that IL-1β and IL-23 had important synergy
191 for pathogenicity (Fig. 4J). In addition, IL-1β greatly expanded RORγt expression in CCR6$^{high}$ MP CD4$^{+}$ T cells
192 but not CCR6$^{low}$ cells, whereas IL-23 somewhat inhibited the proportion of Ki67-expressing cells, suggesting
193 that IL-1β is important for the proliferation of CCR6$^{high}$ MP CD4$^{+}$ T cells (Fig. 4K). To further confirm the
194 functions of IL-1β and IL-23 in MP CD4$^{+}$ T cells, we performed bulk-RNA seq with bystander-activated MP
195 CD4$^{+}$ T cells exposed to IL-1β and IL-23. In the heatmap DEG analysis, IL-1β increased the expression of
196 proliferation-related gene such as *Mki67* and *cdk2,* whereas IL-23 alone did not have any significant effects on
197 gene expression (Fig. 4L). IL-23 and IL-1β together significantly induced the expression of pathogenic genes
198 such as *Bhlhe40, Il1r1, Csf2*, *Ifng, Il22* and *Il17a*. In support, Gene set enrichment analysis (GSEA) pathway
199 enrichment plot of IL-1β vs. IL-1β and IL-23 demonstrated that the enrichment score for cell proliferation was
200 higher with IL-1β, and the score of the pathogenic Th17 signature with IL-1β and IL-23 was higher than in the
201 control group (Fig. 4M). Through these results, we understand that steady-state CCR6$^{high}$ MP CD4$^{+}$ T cells,
202 which show Th17-like characteristics, are the major bystander-activated cells responding to IL-1β and IL-23,
203 which potentiate the cells' pathogenic character.

204 **CCR6$^{high}$ MP CD4$^{+}$ T cells are encephalitogenic and exacerbate autoimmune neuroinflammation.**

205 To reveal the importance of splenic MP CD4$^{+}$ T cells during an autoimmune disease, we first induced EAE in
206 5-week-old mice, who have a lower proportion of MP CD4$^{+}$ T cells than 10-week-old mice. In this mouse model,
207 we compared the disease severity of control mice with that of those who received an additional adoptive transfer
208 of Treg-deleted MP CD4$^{+}$ T cells from 10-week-old Foxp3-GFP mice. EAE was rapidly induced and progressed
209 by transferring additional MP CD4$^{+}$ T cells from 10-week-old mice, suggesting that MP CD4$^{+}$ T cells could be
210 an important contributor to MOG$_{35-55}$-induced EAE pathogenesis (Fig. S7A). In support, Rag$^{-/-}$ mice that
211 received MOG-TCR transgenic (2D2) naïve CD45.1$^{-}$V$_{\beta}$11$^{+}$CD4$^{+}$ T cells with Treg-deleted MP CD4$^{+}$ T cells
212 (CD45.1$^{+}$CD4$^{+}$) showed a more severe phenotype of EAE than the mice that received only 2D2 T cells (Fig.
213 S7B), suggesting that MP CD4$^{+}$ T cells contribute to the pathogenesis of EAE. Based on our previous results,
214 we hypothesized that CCR6$^{high}$ MP CD4$^{+}$ T cells are the major pathogenic subpopulation contributing to EAE
215 disease progression. To test that hypothesis, we transferred CCR6$^{high}$ and CCR6$^{low}$ MP CD4$^{+}$ T cells
216 (CD45.1$^{+}$CD4$^{+}$) and 2D2 naïve CD4$^{+}$ T cells into Rag$^{-/-}$ mice. The additional transfer of CCR6$^{high}$ MP CD4$^{+}$ T
217 cells exacerbated EAE development compared with 2D2 transfer alone or the transfer of CCR6$^{low}$ MP CD4$^{+}$ T
218 cells (Fig. 5A). Interestingly, the number of transferred MP CD4$^{+}$ T cells that appeared in the spinal cord and
219 brain tissue did not differ between conditions (Fig. 5B). However, CCR6$^{high}$ MP CD4$^{+}$ T cells produced
220 significantly more cytokines, particularly IL-17A and GM-CSF, in the spinal cord and brain tissue than CCR6$^{low}$
221 MP CD4$^{+}$ T cells (Fig. 5C and D). Therefore, CCR6$^{high}$ MP CD4$^{+}$ T cells, along with antigen-specific T cells,
222 contribute to the pathogenicity of autoimmune neuroinflammation by expressing pathogenic cytokines such as
223 IL-17A and GM-CSF. To clarify the antigen-independent activation of CCR6$^{high}$ MP CD4$^{+}$ T cells in an EAE
224 mouse model, we detected 2D2 TCR (V$_{\alpha}$3.2$^{+}$ and V$_{\beta}$11$^{+}$), which are predominantly expressed in 2D2 naïve

225 $CD4^+$ T cells. Indeed, $CCR6^{high}$ MP $CD4^+$ T cells barely expressed $V_\alpha3.2^+$ and $V_\beta11^+$ (Fig. 5E and F). In support,
226 we confirmed that steady-state MP $CD4^+$ T cells did not respond to the $MOG_{35-55}$ antigen (Fig. 5G). Collectively,
227 these results suggest that $CCR6^{high}$ MP $CD4^+$ T cells are encephalitogenic cells that exacerbate autoimmune
228 neuroinflammation by producing IL-17A and GM-CSF, presumably in a bystander manner, along with antigen-
229 specific T cells.

230 **Bhlhe40 confers pathogenic functions of bystander $CCR6^{high}$ MP $CD4^+$ T cells by IL-1 and IL-23**

231 Among the candidate genes involved in bystander activation of $CCR6^{high}$ MP $CD4^+$ T cells, we identified that
232 Bhlhe40/GM-CSF axis could potentially give rise to the pathogenic function of $CCR6^{high}$ MP $CD4^+$ T cells
233 induced by IL-1β and IL-23 without TCR stimulation (Fig. 6A). By using $Bhlhe40^{GFP}$ mice, we found that
234 $CCR6^{high}$ MP $CD4^+$ T cells activated by IL-1β and IL-23 showed significantly increased level of Bhlhe40 (Fig.
235 6B). Interestingly, $Bhlhe40^{GFP}$ positive T cells majorly produced effector cytokines including IL-17A and GM-
236 CSF compared to $Bhlhe40^{GFP}$ negative T cells (Fig. 6C). In support, $Bhlhe40^{-/-}$ $CCR6^{high}$ MP $CD4^+$ T cells
237 showed markedly reduced IL-17A and GM-CSF production compared to WT (Fig. 6D and E), suggesting that
238 Bhlhe40 is an important transcriptional regulator for the pathogenic functions of bystander $CCR6^{high}$ MP $CD4^+$
239 T cells. To confirm the in vivo relevance, we transferred WT $CCR6^{high}$ or $Bhlhe40^{-/-}$ $CCR6^{high}$ MP $CD4^+$ T cells
240 along with 2D2 naïve $CD4^+$ T cells into $Rag^{-/-}$ mice. $Bhlhe40^{-/-}$ $CCR6^{high}$ MP $CD4^+$ T cells showed abrogated
241 functions for exacerbating EAE disease compared by WT $CCR6^{high}$ MP $CD4^+$ T cells (Fig. 6F). Interestingly,
242 the number of $Bhlhe40^{-/-}$ $CCR6^{high}$ MP $CD4^+$ T cells expressing IL-17A and GM-CSF in the spinal cord and
243 brain tissue was significantly reduced compared to WT $CCR6^{high}$ MP $CD4^+$ T cells (Fig. 6G and H) without
244 significant difference of MOG-specific 2D2 T cells (data not shown). In addition, transfer of GM-CSF-deficient
245 $CCR6^{high}$ MP $CD4^+$ T cells showed abrogated function of contributing EAE pathogenesis (Fig. 6I), suggesting
246 that disease aggravation by bystander $CCR6^{high}$ MP $CD4^+$ T cells is committed by IL-1β and IL-23 via
247 Bhlhe40/GM-CSF axis. Collectively, these results indicate that Bhlhe40 confers pathogenic functions of
248 bystander $CCR6^{high}$ MP $CD4^+$ T cells with GM-CSF production.

249 **Discussion**

250 In this study, we intensively validated the characteristics of MP conventional $CD4^+$ T cells using scRNA-seq to
251 unveil their effector functions during autoimmune disease. We found distinct effector-like subpopulations in
252 steady-state splenic MP $CD4^+$ T cells that are independent of the microbiome and food antigens. Moreover, MP
253 $CD4^+$ T cells can be bystander-activated toward Th1-, Th2-, and Th17-like effector cells by the IL-1 family and
254 STAT activating cytokines. In particular, chemokine receptor–expressing cells are defined as potential
255 responder cells, and we focused on $CCR6^{high}$ MP $CD4^+$ T cells to further validate their functions in responding
256 to IL-1β/IL-23. We demonstrated that encephalitogenic $CCR6^{high}$ MP conventional $CD4^+$ T cells are bystanders
257 that exacerbate EAE disease progression, along with antigen-specific T cells. Furthermore, we suggested
258 Bhlhe40 as a pivotal transcriptional regulator that governs GM-CSF production by $CCR6^{high}$ MP $CD4^+$ T cells,
259 exacerbating EAE development. Overall, our results reveal the immunological function of antigen-unrelated
260 MP $CD4^+$ T cells in autoimmune disease.

261 According to previous reports, CD44$^{high}$ MP CD4$^{+}$ and CD8$^{+}$ conventional T cells exist spontaneously
262 in mouse spleens, independently of germ and food antigens, and also in humans (Byrne *et al.*, 1994; Haluszczak
263 *et al.*, 2009; Kawabe *et al.*, 2017; Szabolcs *et al.*, 2003). In support, we and others confirmed that MP CD4$^{+}$ T
264 cells are found in mice even 1-2 days after birth and that they increase significantly with age in both the spleen
265 and other tissues (Kawabe *et al.*, 2017). However, the generation of MP CD8$^{+}$ T cells remains controversial.
266 Some studies have reported that MP CD8$^{+}$ T cells are derived from naïve T cells in lymphopenic conditions
267 (Haluszczak *et al.*, 2009; Hamilton *et al.*, 2006; Seddon *et al*, 2000; White *et al.*, 2016), whereas other groups
268 have shown that MP CD8$^{+}$ T cell generation is a TCR-related process triggered by the recognition of self-
269 antigens in the thymus (Miller *et al*, 2020). Along the same lines, MP CD4$^{+}$ T cells have recently been reported
270 to differentiate from naïve CD4$^{+}$ T cells in the periphery in both neonates and adult mice in a thymus-
271 independent fashion (Kawabe *et al.*, 2017). However, it has been recently reported that there is a proportion of
272 memory CD4$^{+}$ T cells in human thymus by scRNA-seq (Park *et al*, 2020), suggesting the potential generation
273 of natural MP T cells. In support, we observed a significant proportion and number of CD44$^{high}$ MP CD4$^{+}$ T
274 cells in the mouse thymus that increased with age. Collectively, therefore, these studies do not rule out the
275 possibility that MP CD4$^{+}$ T cells might be generated both from naïve T cells and directly by the thymus.
276 Furthermore, we found that the TCR diversity of steady-state MP CD4$^{+}$ T cells was slightly reduced in GF mice,
277 revealing that the gut microbiome potentially contributes to certain minor TCR clonotypes of peripheral MP
278 CD4$^{+}$ T cells. In the mLNs, Th17-like MP CD4$^{+}$ T cells were significantly reduced in GF-housed mice,
279 suggesting the importance of the microbiome to gut Th17 cells. Therefore, peripheral self-antigens and the gut
280 microbiome might both contribute to TCR diversity and the proportion of MP CD4$^{+}$ T cells.

281 The heterogeneous characteristics of MP conventional CD4$^{+}$ T cells were investigated using single cell
282 transcriptomics, which revealed clearly distinct Th1-, Th17-, Tfh-, and Treg-like subpopulations. In support,
283 recent studies revealed the potential heterogeneity of murine MP CD4$^{+}$ T cells (ElTanbouly *et al*, 2020; Kawabe
284 *et al*, 2020) and further demonstrated that a CXCR3$^{+}$T-bet$^{+}$ Th1-like MP population was differentiated from
285 naïve CD4$^{+}$ T cells by DC1-derived IL-12 and further activated by CD40–CD40L interactions between DC1
286 and CD4$^{+}$ T cells (Kawabe *et al.*, 2020). Of note, MP CD4$^{+}$ and CD8$^{+}$ T cells rapidly produce IFN-γ in response
287 to IL-12 and IL-18 (Guo *et al*, 2009; Kawabe *et al.*, 2017; Sosinowski *et al.*, 2013; White *et al.*, 2017). Given
288 those observations, we hypothesized that CXCR3$^{high}$ MP CD4$^{+}$ T cells are major responders to IL-12 and IL-18
289 cytokine stimulation. As expected, we confirmed that CXCR3$^{high}$ MP CD4$^{+}$ T cells, in high correlation with
290 CCR5 expression, can produce IFN-γ and T-bet in response to IL-12 and IL-18, suggesting a potential innate-
291 like function of CXCR3$^{high}$ MP CD4$^{+}$ T cells. Interestingly, without TCR stimulation, cytokine-mediated
292 bystander activation could not induce TNF-α from MP CD4$^{+}$ T cells, suggesting that TCR and cytokine
293 signaling produce distinct effector functions. We also used IL-33 and IL-25 stimulation of MP CD4$^{+}$ T cells to
294 see whether they produced Th2 cytokines such as IL-13 and IL-5. Interestingly, the MP CD4$^{+}$ T cells produced
295 IL-4 with TCR stimulation, suggesting that the effector function of MP CD4$^{+}$ T cells bystander-activated by IL-
296 33 and IL-25 correlates with innate lymphoid cell type 2 (ILC2). A previous report consistently showed that *in*
297 *vitro*–generated memory Th2 cells mainly produce IL-13, rather than IL-4, upon exposure to IL-33 and IL-7
298 without a cognate antigen. In addition, like ILC2, tissue-resident memory Th2 cells were activated by IL-33 and

299 showed a protective function against helminth infection in an antigen-independent manner (Guo *et al*, 2015).
300 Although we did not observe a significant Th2-like MP subpopulation in the steady state, we confirmed that
301 Th2-like populations are induced by IL-33 and IL-25, suggesting that heterogeneous IL-33R- or IL-25R-
302 expressing cells might be responding to those cytokines.

303 In our previous study, we demonstrated that and IL-23 can synergistically potentiate the pathogenicity
304 of memory $CD4^+$ T cells *in vitro* (Lee *et al.*, 2019) and that non-myelin-specific $CD4^+$ T cells can infiltrate the
305 CNS with MOG antigen–specific T cells, which significantly contribute to EAE disease progression (Jones *et*
306 *al.*, 2003; Lee *et al.*, 2019). In rheumatoid arthritis patients, T cells that infiltrate the synovial fluid mainly
307 express the $CD45RO^+$ memory marker and specifically respond to epitopes of Epstein-Barr virus and
308 cytomegalovirus (Kobayashi *et al.*, 2004; Pacheco *et al*, 2019; Scotet *et al*, 1999; Tan *et al.*, 2000). In type 1
309 diabetes, infection with rotavirus or coxsackie virus is reported to be involved in accelerated diabetes onset
310 through Toll-like receptor (TLR) signaling without pancreatic infection (Horwitz *et al*, 1998; Pane *et al*, 2014),
311 and influenza A virus is linked to diabetes in human patients (Nenna *et al*, 2011; Pane & Coulson, 2015).
312 Collectively, those studies suggest that antigen-non-related $CD4^+$ T cells can contribute to disease onset or
313 progression with antigen-specific T cells in various autoimmune diseases. We have identified here that $CCR6^{high}$
314 MP $CD4^+$ T cells are the major subpopulation of MP $CD4^+$ T cells that respond to IL-1β and IL-23 by expanding
315 and inducing pathogenic Th17 characteristics. In an adoptive transfer model of EAE, $CCR6^{high}$ MP $CD4^+$ T cells
316 transferred with MOG-specific T cells induced more severe EAE than $CCR6^{low}$ cells, with increased production
317 of IL-17 and GM-CSF in the CNS. We further confirmed that MP $CD4^+$ T cells do not respond to $MOG_{33-55}$
318 antigen, indicating the bystander role of $CCR6^{high}$ MP $CD4^+$ T cells in autoimmune neuroinflammation. Because
319 MOG-specific T cells produce effector cytokines such as IL-17 and GM-CSF (data not shown), further studies
320 should be done to reveal the distinct mechanism between antigen-specific T cells and bystander-activated T
321 cells in autoimmune disease pathogenesis.

322 Analyzing the single cell transcriptomics of IL-1β/IL-23 responding MP $CD4^+$ T cells, we identified
323 that Bhlhe40 could be a potential transcriptional regulator inducing GM-CSF in $CCR6^{high}$ MP $CD4^+$ T cells.
324 Bhlhe40 has been reported to play pivotal roles in T cells. Bhlhe40-deficient naïve $CD4^+$ T cells show limited
325 response to TCR stimulation (Martinez-Llordella *et al*, 2013). Moreover, Bhlhe40 seem to be required for Th1
326 and Th17 effector cytokine production including IL-17A, GM-CSF and IFN-γ in the context of autoimmune
327 disease, GVHD, and Toxoplasma gondii infection model (Lin *et al.*, 2016; Lin *et al*, 2014; Piper *et al*, 2020; Yu
328 *et al*, 2018). In addition, a binding site for Bhlhe40 was identified the correlation of mouse *Csf2* locus, which
329 encodes GM-CSF, (Jarjour *et al*, 2020; Lin *et al.*, 2014) and Bhlhe40 expression positively correlate with GM-
330 CSF expression in human PBMC (Emming *et al*, 2020). We demonstrate that steady-state $CCR6^{high}$ MP $CD4^+$
331 T cells have Th17-like character with expressing RORγt. They up-regulated Bhlhe40 in response to IL-1β and
332 IL-23 in the absence of TCR engagement for IL-17 and GM-CSF production. Moreover, transferring these cells
333 in vivo, we found that Bhlhe40 is required in bystander $CCR6^{high}$ MP $CD4^+$ T cells for the expression of GM-
334 CSF contributing to the pathogenesis of EAE development. In support, a previous study reported the majority
335 of Bhlhe40-expressing pathogenic T cells in active EAE are non-MOG-specific (Lin *et al.*, 2016; Lin *et al.*,

336 2014). Therefore, Bhlhe40 can be a pivotal transcriptional regulator for both antigen-specific and bystander MP
337 T cells in the context of CNS inflammation and targeting of Bhlhe40 in $CD4^+$ T cells may serve as a potential
338 novel treatment strategy to control autoimmune diseases.

339 Innate T cells such as natural killer T (NKT), mucosal-associated invariant T (MAIT), and γδ T cells
340 have limited TCR gene usage compared to conventional T cells, which recognize complexes of non-peptide
341 antigens such as glycolipids, phosphoantigens, and vitamin B metabolites, respectively (Godfrey *et al*, 2015;
342 Lee *et al*, 2020; Pellicci *et al*, 2020). These innate T cells are derived from the thymus, which can evoke robust
343 cytokine production. Previously, innate lymphocytes, such as NKT17, γδT17 cell, and ILC3 subsets have been
344 defined to commonly express IL-17 and RORγt (Lee *et al*, 2013b; Sutton *et al*, 2009; Walker *et al*, 2013).
345 Furthermore, a recent study reported a novel subset of αβ-γδ co-expressing T cells which recognize MHC-
346 restricted peptide antigens and produce effector cytokine IL-17A, GM-CSF, and IFN-γ by IL-1β and IL-23
347 stimulation (Edwards *et al*, 2020). In this context, we carefully eliminated the possibility of contamination of
348 innate T cells by sorting conventional MP $CD4^+$ T cells using NKT (CD1d tetramer), γδ T, αβ-γδ T, ILC, and
349 MAIT ($TCR\beta^+CD8^-CD4^+CD25^-CD44^{high}CD62L^{low}$) exclusion gates. We confirmed that PLZF/CD1d tetramer
350 negative steady-state MP $CD4^+$ T cells still exists as a heterogenous population containing $CCR6^{high}ROR\gamma t^+IL-$
351 $17A^+$ cells, which is majorly bystander-activated by IL-1β and IL-23. Therefore, collectively, we provide
352 compelling evidence that conventional $CD4^+$ T cells distinguished from previously known innate T cells exist,
353 which have an innate-like features and contribute to autoimmune neuroinflammation.

354 Memory T cells are antigen-experienced cells that respond to their cognate antigens more rapidly upon
355 re-exposure. Therefore, we speculate that MP $CD4^+$ T cells would have antigen-specific memory responses, and
356 we wonder what the antigen is. Previous studies showed that antigen-specific cells called virtual memory cells
357 exist without antigen exposure and nonetheless perform the memory response. For example, *vaccinia* virus
358 B8R- and HSV-specific MP $CD8^+$ T cells in unimmunized mice can react to those specific antigens (Haluszczak
359 *et al.*, 2009; Hamilton *et al.*, 2006). Virtual memory $CD8^+$ T cells have a $CD44^{high}CD122^+CD49d^{low}$ phenotype
360 which requires a transcription factor *Eomes* that differs from that of antigen-induced memory cells (Sosinowski
361 *et al.*, 2013). In addition, virus-specific MP $CD4^+$ T cells are abundant in unexposed adults, presumably through
362 cross-reactivity, so that they have the typical properties of memory T cells (Su & Davis, 2013; Su *et al*, 2013).
363 However, virtual memory $CD8^+$ T cells are also known to play a protective role in infection using an antigen-
364 non-specific manner (White *et al.*, 2016). Therefore, MP $CD4^+$ T cells derived from steady-state mice might
365 have cross-reactivity to certain pathogens even though they did not respond to the $MOG_{35-55}$ antigen *in vitro*,
366 and we speculate that they have both antigen-specific and bystander functions.

367 Antigen-specific T cells are fundamentally important in triggering autoimmune inflammation;
368 however, antigen-non-related MP $CD4^+$ T cells also contribute to pathogenic inflammation in a bystander
369 manner. Collectively, our studies of the role that MP $CD4^+$ T cells play in neuroinflammatory disease shed light
370 on the innate-like function of adaptive immune cells to understand disease pathogenesis and reveal a novel drug
371 development strategy to modulate autoimmune diseases.

372 **Experimental and Methods**

373 **Mice**

374 C57BL/6J mice were purchased from DBL (Chungcheongbuk-do, Korea), and Rag$^{-/-}$ , GM-CSF$^{-/-}$ and 2D2
375 TCR-transgenic mice were purchased from Jackson Laboratory (Bar Harbor, ME, USA). CD45.1$^{+}$, Foxp3-GFP
376 mice were provided by Jeehee Youn (Hanyang University). GF and AF mice were purchased from the animal
377 facility of POSTECH Biotech Center (Pohang, Korea). Bhlhe40$^{-/-}$ and Bhlhe40$^{GFP}$ mice were provided by Brian
378 T. Edelson (Washington University). The mice were housed and bred in a specific pathogen–free animal facility
379 at Hanyang University under controlled conditions with a constant temperature (21 ± 1 °C) and humidity
380 (50 ± 5%) and a 12 h light/dark cycle with regular chow and autoclaved water.

381 **Cell isolation and differentiation**

382 MP (TCRβ$^{+}$CD4$^{+}$CD1d tetramer$^{-}$CD25$^{-}$CD62L$^{low}$CD44$^{high}$) CD4$^{+}$ T cells from the spleens of 8 to 12-week-old
383 mice were isolated using a FACS Aria cell sorter II (BD Biosciences, Franklin Lakes, NJ, USA). FACS-sorted
384 MP CD4$^{+}$ T cells were stimulated with IL-1β (20 ng/mL, R&D Systems, Minneapolis, MN, USA), IL-23 (20
385 ng/mL, R&D Systems), IL-12 (20 ng/mL, Peprotech, Rocky Hill, NJ, USA), IL-18 (20 ng/mL, R&D Systems),
386 IL-33 (20 ng/mL, R&D Systems), IL-25 (20 ng/mL, R&D Systems), IL-7 (10 ng/mL, Peprotech, Rocky Hill,
387 NJ, USA), or plate-bound anti-CD3/anti-CD28 (2 μg/mL, BD Biosciences) for 5 days at 37 °C in an incubator.

388 **Flow cytometry**

389 Cell surface staining was performed using the following monoclonal antibodies: anti-CD4 (RM4-5;
390 eBioscience, San Diego, CA, USA, dilution 1:500), anti-CD25 (PC61.5; eBioscience, dilution 1:500), anti-
391 CD44 (IM7; BioLegend, San Diego, CA, USA, dilution 1:500), anti-CD62L (MEL-14; BioLegend, dilution
392 1:500), anti-CD45 (30-F11, BioLegend, dilution 1:500), anti-CD45.1 (A20; eBioscience, dilution 1:500), anti-
393 TCRβ (H57-597; eBioscience, dilution 1:500), anti-CCR6 (29-2L17; BD, dilution 1:100), anti-CXCR3
394 (CXCR3-173; BD, dilution 1:100), anti-V$_{\alpha}$3.2 (RR3-16; BioLegend, dilution 1:500), anti-V$_{\beta}$11 (RR3-15;
395 BioLegend, dilution 1:500), and PE-conjugated CD1d tetramer (PBS57; NIH, dilution 1:1000). Biotinylated
396 PBS57 loaded and unloaded CD1d monomers were provided by the US National Institutes of Health Tetramer
397 Core facility. For intracellular staining, the cells were stimulated with a cell stimulation cocktail (00-4975-03;
398 eBioscience) for 4 h at 37 °C, and then surface markers were stained. After staining of the surface markers, the
399 cells were fixed and permeabilized in Cytofix/Cytoperm (554714; BD Bioscience) or FOXP3/Transcription
400 factor staining buffer set (00-5523-00; eBioscience) for 30 min at 4 °C or RT. Intracellular staining was
401 performed using the following monoclonal antibodies: anti-IL-17A (eBio17B7; eBioscience, dilution 1:200),
402 anti-IFN-γ (XMG1.2; eBioscience, dilution 1:400), anti-GM-CSF (MP1-22E9; BD Biosciences, dilution 1:200),
403 anti-Ki67 (SolA15; eBioscience, dilution 1:500), anti-IL-4 (11B11; BioLegend, dilution 1:200), IL-13
404 (eBio13A; eBioscience, dilution 1:200), anti-TNF-α (MP6-XT22; BioLegend, dilution 1:500), anti-IL-5
405 (TRFK5; BioLegend, dilution 1:200), anti-IL-1R1 (35F5; BD Biosciences, dilution 1:100), anti-RORγt (Q31-

378; BD Biosciences, dilution 1:100), anti-T-bet (4B10; BioLegend, dilution 1:50), anti-GATA3 (L50-823; BD Bioscience, dilution 3 μl per well) and IgG1 (R2-34; BD Biosciences). Stained cells were analyzed by flow cytometry (FACS Canto II, BD Bioscience), and data were analyzed using FlowJo software version 10.8.0 (Tree Star, Ashland, OR, USA).

**Experimental autoimmune encephalomyelitis**

In EAE model, FACS-sorted MP $CD4^+$ T cells ($TCR\beta^+CD4^+CD1d$ $tetramer^-Foxp3^-CD62L^{low}CD44^{high}$, $5 \times 10^5$) from Foxp3-GFP mice were adoptively transferred to 5-week-old female C57BL/6 mice. After transfer, the mice were immunized with 200 μg of $MOG_{35\text{-}55}$ peptide in complete Freund's adjuvant (Chondrex, Inc., USA). At 0 and 48 h after immunization, the mice were intraperitoneally treated with 500 ng of pertussis toxin (List Biological Laboratories, Inc., Campbell, CA, USA). The animals were scored daily for clinical disease. In another EAE model by adoptive transfer, naive ($CD4^+V_\beta11^+CD25^-CD62L^{high}CD44^{low}$) $CD45.1^-$ T cells (1-5 × $10^4$) from 2D2 TCR-transgenic mice were transferred into $Rag^{-/-}$ mice with or without WT $CCR6^{high}$ or WT $CCR6^{low}$ or $Bhlhe40^{-/-}$ $CCR6^{high}$ or $GM\text{-}CSF^{-/-}$ $CCR6^{high}$ or $GM\text{-}CSF^{-/-}$ $CCR6^{low}$ MP $CD4^+$ T cells ($1.0 \times 10^5$). Before transfer, $CCR6^{high}$ or $CCR6^{low}$ MP $CD4^+$ T cells were primed *in vitro* with IL-7 (10 ng/mL) and IL-1β (20 ng/mL) for 5–7 days. After transfer, the mice were immunized with 100 μg of $MOG_{35–55}$ peptide in complete Freund's adjuvant (Chondrex, Inc., USA). At 0 and 48 h after immunization, the mice were intraperitoneally treated with 200 ng of pertussis toxin (List Biological Laboratories, Inc., Campbell, CA, USA). The animals were scored daily for clinical disease as follows (Stromnes & Goverman, 2006): partially limp tail, 0.5; completely limp tail, 1; limp tail and waddling gait, 1.5; paralysis of one hind limb, 2; paralysis of one hind limb and partial paralysis of the other hind limb, 2.5; paralysis of both hind limbs, 3; ascending paralysis, 3.5; paralysis of trunk, 4; moribund, 4.5; dead, 5. On day 12 or 13, the mice were sacrificed and perfused with Phosphate buffered saline (PBS). To isolate lymphocytes, the spinal cord and brain were digested with 1 mg/mL of collagenase D (11 088 866 001; Sigma-Aldrich) and DNase I (10 104 159 001; Sigma-Aldrich) and incubated at 80 RPM on a shaker for 35 min. After enzyme digestion, lymphocytes were isolated by Percoll (GE Healthcare, Little Chalfont, UK) density-gradient centrifugation.

**T cell proliferation and cytokine assays**

For antigen-specific proliferation, 2D2 naïve ($CD4^+V_\beta11^+CD25^-CD62L^{high}CD44^{low}$) and MP $CD4^+$ T cells ($CD4^+CD25^-CD62L^{low}CD44^{high}$) and $CD11c^+$ dendritic cells ($MHC\text{-}II^+CD11c^+$) (APC) from the spleens of 2D2 TCR-transgenic and C57BL/6 mice were isolated using a FACS Aria cell sorter II. Before co-culture, naïve and MP $CD4^+$ T cells were stained with 1.25 μM carboxyfluorescein succinimidyl ester (CFSE) (Invitrogen, Carlsbad, CA) for 7 min at room temperature. After incubation, 10% Fetal bovine serum (FBS) was added, and the incubation was continued on ice for 3 min. 2D2 Naïve and MP $CD4^+$ T cells ($1 \times 10^5$ cells/well) were then washed with PBS and co-cultured with $CD11c^+$ dendritic cells ($5 \times 10^4$) with or without 50 μg/mL of $MOG_{35\text{-}55}$ peptide for 72 h.

440 **Enzyme-linked immunosorbent assay (ELISA)**

441 Samples were measured using IL-17A ELISA (432501; BioLegend), IL-13 ELISA (88-7137-88; Thermo
442 Fisher), IL-4 ELISA (431104; BioLegend), IL-5 ELISA (431204; BioLegend), IFN-γ ELISA (430801;
443 BioLegend), TNF-α ELISA (430904; BioLegend), and GM-CSF ELISA (432201; BioLegend) kits according
444 to the manufacturers' instructions. Briefly, microwell plates (Corning Costar; 9018) were coated with capture
445 antibodies overnight at 4 °C and blocked with ELISA diluent 1X for 1 h at room temperature. Samples and two-
446 fold serial diluted standards were incubated at room temperature for 2 h, and then detection antibodies and
447 streptavidin-HRP were added. Then, 1X TMB solution and a stop solution (2 N $H_2SO_4$) was loaded. The optical
448 density was analyzed at 450 nm. Between all procedures, plates were washed at least 3 times with wash buffer
449 (1X PBS, 0.05% Tween-20).

450 **Statistical analysis**

451 All data were analyzed in non-parametric analyses using the Mann-Whitney test or two-way ANOVA of
452 variance in Prism version 8.0 (GraphPad Software, San Diego, CA). Data are presented as the mean ± S.D. or
453 mean ± S.E.M. For all data, significance was defined as $p \leq 0.05$. Sample size and statistical information is
454 provided in each figure legend.

455 **Single-cell RNA sequencing sample preparation**

456 MP ($TCR\beta^{+}CD4^{+}CD25^{-}CD62L^{low}CD44^{high}$) $CD4^{+}$ T cells from the spleens of 10-week-old mice were isolated
457 using a FACS Aria cell sorter II (BD Biosciences, Franklin Lakes, NJ, USA). FACS-sorted MP $CD4^{+}$ T cells
458 were stimulated with IL-1β (20 ng/mL, R&D Systems, Minneapolis, MN, USA), IL-23 (20 ng/mL, R&D
459 Systems), IL-12 (20 ng/mL, Peprotech, Rocky Hill, NJ, USA), IL-18 (20 ng/mL, R&D Systems), IL-33 (20
460 ng/mL, R&D Systems), IL-25 (20 ng/mL, R&D Systems), or IL-7 (10 ng/mL, Peprotech, Rocky Hill, NJ, USA)
461 for 5 days at 37 °C in an incubator.

462 **Single-cell RNA- and TCR-seq data processing**

463 Raw sequencing data were processed using a well-developed program, Cellranger (10X genomics), for quality
464 control (QC) and gene expression estimation. Low-quality cells were filtered using 4 QC metrics: the percentage
465 of mitochondrial gene unique molecular identifier (UMI) counts, the number of expressed genes (UMI count >
466 0), the sum of UMI counts per cell, and the doublet score estimated using Doublet Finder
467 [10.1016/j.cels.2019.03.003]. The outlier cells from each QC metric were excluded from further analyses. To
468 collect pure $TCR\alpha/\beta^{+}$ $CD4^{+}$ T cells, cells expressing PLZF (*Zbtb16*) and *Cd74*$^{+}$-cells in which at least 1 UMI
469 was counted were removed. All $TCR\alpha/\beta^{+}$ $CD4^{+}$T cells were integrated by cytokine treatment (set 1: IL-7, IL-
470 7+ IL-1β, and IL-7+ IL-1β +IL-23; set 2: IL7, IL7+IL-25, IL-7+IL-33, and IL-7+IL-25+IL-33; set 3: IL-7, IL-
471 7+IL-12, IL-7+IL-18, and IL-7+IL-12+IL-18) using monocle3 [10.1038/nmeth.4402]. TCR-seq raw sequencing
472 data were processed using the Cellranger 'adj' program. The TCR clonotypes from previously filtered scRNA-
473 seq were used in the further analyses.

474 **Single-cell RNA-seq data analysis**

475 The preprocessed scRNA-seq data were aligned with the IL-7 treatment group using 'align_cds' from the
476 monocle3 program [https://doi.org/10.1038/s41586-019-0969-x], and data were integrated for each set. Each
477 cluster was characterized using the marker gene expression levels and referring to previous studies. The top
478 specifically expressed genes of each cluster were selected by the specificity of each gene, as estimated using
479 'FindAllMarkers' in Seurat v4.0 [https://doi.org/10.1016/j.cell.2021.04.048], and then their expression level
480 was visualized using 'DoHeatmap' in the same program. We calculated the percentage of cells in each condition
481 for each cell type by dividing the number of cells in each condition by the number of clustered cells. A DEGs
482 analysis was performed for each cytokine treatment of each set using 'FindMarkers' in Seurat with the following
483 parameters: min.pct = 0, min.cells.feature = 1, min.cells.group = 1, logfc.threshold = 0. DEGs between cytokine
484 treatments and DEGs between conditions were defined at FDR <0.05 and average log2 fold change ≥0.1. A
485 functional analysis of DEGs and cluster specific gene sets was performed in MSigDB's C2 (KEGG) and C5
486 (GO). The functions were analyzed using the maximum and minimum size of the gene sets (KEGG with min 2
487 genes and max 500, GO with min 2 genes and max 150 genes). The gene set enrichment test was performed
488 using the 'enricher' function of the clusterProfile package [10.1089/omi.2011.0118]. The significance level was
489 set as the function that satisfied FDR < 0.2 and had at least 2 overlapping genes.

490 **Signature score of the MP $CD4^+$ T cells**

491 The signature score of the $CD4^+$ T cells was estimated to define the features of each cell type. The monocle3
492 object of each set of cytokine treatments was transformed into the Seurat object. They were normalized by
493 condition and then integrated. The signature score of each cell type was calculated using AddModuleScore in
494 the Seurat package.

495 **Trajectory inference of MP $CD4^+$ T cells by cytokine stimulation**

496 Effector memory $CD4^+$ T-cells have the plasticity to differentiate into various helper cells. We performed a
497 trajectory analysis on the subcluster composed of the initial cells that are likely to be differentiated according to
498 each cytokine stimulus and the cells that responded. First, we selected 2,000 highly variable genes by cell type,
499 and then we inferred the trajectory using reduceDimension with DDRTree in the monocle2 program
500 [10.1038/nbt.2859]. Pseudo-time was calculate using orderCells in the same program. DEGs following the
501 pseudo-time trajectory were defined at a q-value < 1e-50.

502 **Estimation of regulon activity score**

503 *Regulon* describes the relationship between a transcription factor and its regulatory target genes, and its activity
504 is calculated using the expression levels of the genes in the regulon. First, we constructed a correlation matrix
505 between genes, and then we calculated the activity of each regulon using GENIE3
506 [10.1371/journal.pone.0012776]. At that time, all the parameters were set to the default. The regulon
507 relationship was derived from mm10__refseq-r80__500bp_up_and_100bp_down_tss.mc9nr and
508 mm10__refseq-r80__10kb_up_and_down_tss.mc9nr in the 'cisTarget_databases' of the R package. All

processes were performed using the SCENIC program in R [10.1038/nmeth.4463]. Differentially activated regulons were considered only when they contained at least 1% of expressing cells.

**T-cell receptor repertoire analysis**

The TCR repertoire of the cells was considered only from the scRNA-seq data. The degree of TCR expansion was categorized as hyperexpanded (100 < X <= 500), large (20 < X <= 100), medium (5 < X <= 20), small (1 < X <= 5), and single (0 < X <= 1). The TCR diversity of each sample was calculated using Shannon's index, which considers non-uniformity in the frequency of the clonotype (gene and nucleotide sequences). All procedures were performed using scRepertoire [10.12688/f1000research.22139.2] in R.

**SUPPLEMENTARY MATERIALS**

Fig. S1. $CD44^{high}$ memory phenotype (MP) $CD4^+$ T cells increase with age in mice.

Fig. S2. Strategy and flow of single cell RNA-sequencing analysis.

Fig. S3. KEGG/GO analysis of steady-state MP $CD4^+$ T cells.

Fig. S4. Effector T cell lineage–specific marker expression in MP $CD4^+$ T cells.

Fig. S5. Comparison of MP $CD4^+$ T cells in tissues from SPF, GF, and AF mice.

Fig. S6. Effector T cell lineage–specific chemokine receptors and transcription factors in MP $CD4^+$ T cells from SPF and GF mice.

Fig. S7. MP $CD4^+$ T cells exacerbate autoimmune encephalomyelitis.

529 **REFERENCES AND NOTES**


530 Akue AD, Lee JY, Jameson SC (2012) Derivation and maintenance of virtual memory CD8 T cells.
531 *J Immunol* 188: 2516-2523
532 Brennan FM, Smith NM, Owen S, Li C, Amjadi P, Green P, Andersson A, Palfreeman AC, Hillyer P,
533 Foey A *et al* (2008) Resting CD4+ effector memory T cells are precursors of bystander-activated
534 effectors: a surrogate model of rheumatoid arthritis synovial T-cell function. *Arthritis Res Ther* 10:
535 R36
536 Byrne JA, Stankovic AK, Cooper MD (1994) A novel subpopulation of primed T cells in the human
537 fetus. *J Immunol* 152: 3098-3106
538 Cho BK, Rao VP, Ge Q, Eisen HN, Chen J (2000) Homeostasis-stimulated proliferation drives naive
539 T cells to differentiate directly into memory T cells. *J Exp Med* 192: 549-556
540 Chu T, Tyznik AJ, Roepke S, Berkley AM, Woodward-Davis A, Pattacini L, Bevan MJ, Zehn D, Prlic
541 M (2013) Bystander-activated memory CD8 T cells control early pathogen load in an innate-like,
542 NKG2D-dependent manner. *Cell Rep* 3: 701-708
543 Dobber R, Hertogh-Huijbregts A, Rozing J, Bottomly K, Nagelkerken L (1992) The involvement of
544 the intestinal microflora in the expansion of CD4+ T cells with a naive phenotype in the periphery.
545 *Dev Immunol* 2: 141-150
546 Edwards SC, Sutton CE, Ladell K, Grant EJ, McLaren JE, Roche F, Dash P, Apiwattanakul N, Awad
547 W, Miners KL *et al* (2020) A population of proinflammatory T cells coexpresses alphabeta and
548 gammadelta T cell receptors in mice and humans. *J Exp Med* 217
549 ElTanbouly MA, Zhao Y, Nowak E, Li J, Schaafsma E, Le Mercier I, Ceeraz S, Lines JL, Peng C,
550 Carriere C *et al* (2020) VISTA is a checkpoint regulator for naive T cell quiescence and peripheral
551 tolerance. *Science* 367
552 Emming S, Bianchi N, Polletti S, Balestrieri C, Leoni C, Montagner S, Chirichella M, Delaleu N,
553 Natoli G, Monticelli S (2020) A molecular network regulating the proinflammatory phenotype of
554 human memory T lymphocytes. *Nat Immunol* 21: 388-399
555 Ernst B, Lee DS, Chang JM, Sprent J, Surh CD (1999) The peptide ligands mediating positive
556 selection in the thymus control T cell survival and homeostatic proliferation in the periphery.
557 *Immunity* 11: 173-181
558 Godfrey DI, Uldrich AP, McCluskey J, Rossjohn J, Moody DB (2015) The burgeoning family of
559 unconventional T cells. *Nat Immunol* 16: 1114-1123
560 Goldrath AW, Bevan MJ (1999) Low-affinity ligands for the TCR drive proliferation of mature CD8+
561 T cells in lymphopenic hosts. *Immunity* 11: 183-190
562 Goldrath AW, Luckey CJ, Park R, Benoist C, Mathis D (2004) The molecular program induced in T
563 cells undergoing homeostatic proliferation. *Proc Natl Acad Sci U S A* 101: 16885-16890
564 Guo L, Huang Y, Chen X, Hu-Li J, Urban JF, Jr., Paul WE (2015) Innate immunological function of
565 TH2 cells in vivo. *Nat Immunol* 16: 1051-1059

566 Guo L, Wei G, Zhu J, Liao W, Leonard WJ, Zhao K, Paul W (2009) IL-1 family members and STAT
567 activators induce cytokine production by Th2, Th17, and Th1 cells. *Proc Natl Acad Sci U S A* 106:
568 13463-13468
569 Haluszczak C, Akue AD, Hamilton SE, Johnson LD, Pujanauski L, Teodorovic L, Jameson SC, Kedl
570 RM (2009) The antigen-specific CD8+ T cell repertoire in unimmunized mice includes memory
571 phenotype cells bearing markers of homeostatic expansion. *J Exp Med* 206: 435-448
572 Hamilton SE, Wolkers MC, Schoenberger SP, Jameson SC (2006) The generation of protective
573 memory-like CD8+ T cells during homeostatic proliferation requires CD4+ T cells. *Nat Immunol* 7:
574 475-481
575 Hellings N, Baree M, Verhoeven C, D'Hooghe M B, Medaer R, Bernard CC, Raus J, Stinissen P
576 (2001) T-cell reactivity to multiple myelin antigens in multiple sclerosis patients and healthy
577 controls. *J Neurosci Res* 63: 290-302
578 Hemmer B, Vergelli M, Tranquill L, Conlon P, Ling N, McFarland HF, Martin R (1997) Human T-cell
579 response to myelin basic protein peptide (83-99): extensive heterogeneity in antigen recognition,
580 function, and phenotype. *Neurology* 49: 1116-1126
581 Horwitz MS, Bradley LM, Harbertson J, Krahl T, Lee J, Sarvetnick N (1998) Diabetes induced by
582 Coxsackie virus: initiation by bystander damage and not molecular mimicry. *Nat Med* 4: 781-785
583 Jarjour NN, Bradstreet TR, Schwarzkopf EA, Cook ME, Lai CW, Huang SC, Taneja R, Stappenbeck
584 TS, Van Dyken SJ, Urban JF, Jr. *et al* (2020) BHLHE40 Promotes TH2 Cell-Mediated Antihelminth
585 Immunity and Reveals Cooperative CSF2RB Family Cytokines. *J Immunol* 204: 923-932
586 Jones RE, Kay T, Keller T, Bourdette D (2003) Nonmyelin-specific T cells accelerate development
587 of central nervous system APC and increase susceptibility to experimental autoimmune
588 encephalomyelitis. *J Immunol* 170: 831-837
589 Kaech SM, Cui W (2012) Transcriptional control of effector and memory CD8+ T cell differentiation.
590 *Nat Rev Immunol* 12: 749-761
591 Kawabe T, Jankovic D, Kawabe S, Huang Y, Lee PH, Yamane H, Zhu J, Sher A, Germain RN, Paul
592 WE (2017) Memory-phenotype CD4(+) T cells spontaneously generated under steady-state
593 conditions exert innate TH1-like effector function. *Sci Immunol* 2
594 Kawabe T, Yi J, Kawajiri A, Hilligan K, Fang D, Ishii N, Yamane H, Zhu J, Jankovic D, Kim KS *et al*
595 (2020) Requirements for the differentiation of innate T-bet(high) memory-phenotype CD4(+) T
596 lymphocytes under steady state. *Nat Commun* 11: 3366
597 King C, Ilic A, Koelsch K, Sarvetnick N (2004) Homeostatic expansion of T cells during immune
598 insufficiency generates autoimmunity. *Cell* 117: 265-277
599 Koay HF, Gherardin NA, Enders A, Loh L, Mackay LK, Almeida CF, Russ BE, Nold-Petry CA, Nold
600 MF, Bedoui S *et al* (2016) A three-stage intrathymic development pathway for the mucosal-
601 associated invariant T cell lineage. *Nat Immunol* 17: 1300-1311

602 Kobayashi M, Yasui N, Ishimaru N, Arakaki R, Hayashi Y (2004) Development of autoimmune
603 arthritis with aging via bystander T cell activation in the mouse model of Sjogren's syndrome.
604 *Arthritis Rheum* 50: 3974-3984
605 Kondrack RM, Harbertson J, Tan JT, McBreen ME, Surh CD, Bradley LM (2003) Interleukin 7
606 regulates the survival and generation of memory CD4 cells. *J Exp Med* 198: 1797-1806
607 Kovalovsky D, Uche OU, Eladad S, Hobbs RM, Yi W, Alonzo E, Chua K, Eidson M, Kim HJ, Im JS *et*
608 *al* (2008) The BTB-zinc finger transcriptional regulator PLZF controls the development of invariant
609 natural killer T cell effector functions. *Nat Immunol* 9: 1055-1064
610 Le Saout C, Mennechet S, Taylor N, Hernandez J (2008) Memory-like CD8+ and CD4+ T cells
611 cooperate to break peripheral tolerance under lymphopenic conditions. *Proc Natl Acad Sci U S A*
612 105: 19414-19419
613 Lee HG, Lee JU, Kim DH, Lim S, Kang I, Choi JM (2019) Pathogenic function of bystander-activated
614 memory-like CD4(+) T cells in autoimmune encephalomyelitis. *Nat Commun* 10: 709
615 Lee JY, Hamilton SE, Akue AD, Hogquist KA, Jameson SC (2013a) Virtual memory CD8 T cells
616 display unique functional properties. *Proc Natl Acad Sci U S A* 110: 13498-13503
617 Lee M, Lee E, Han SK, Choi YH, Kwon DI, Choi H, Lee K, Park ES, Rha MS, Joo DJ *et al* (2020)
618 Single-cell RNA sequencing identifies shared differentiation paths of mouse thymic innate T cells.
619 *Nat Commun* 11: 4367
620 Lee YJ, Holzapfel KL, Zhu J, Jameson SC, Hogquist KA (2013b) Steady-state production of IL-4
621 modulates immunity in mouse strains and is determined by lineage diversity of iNKT cells. *Nat*
622 *Immunol* 14: 1146-1154
623 Lees JR, Sim J, Russell JH (2010) Encephalitogenic T-cells increase numbers of CNS T-cells
624 regardless of antigen specificity by both increasing T-cell entry and preventing egress. *J*
625 *Neuroimmunol* 220: 10-16
626 Lertmemongkolchai G, Cai G, Hunter CA, Bancroft GJ (2001) Bystander activation of CD8+ T cells
627 contributes to the rapid production of IFN-gamma in response to bacterial pathogens. *J Immunol*
628 166: 1097-1105
629 Lin CC, Bradstreet TR, Schwarzkopf EA, Jarjour NN, Chou C, Archambault AS, Sim J, Zinselmeyer
630 BH, Carrero JA, Wu GF *et al* (2016) IL-1-induced Bhlhe40 identifies pathogenic T helper cells in a
631 model of autoimmune neuroinflammation. *J Exp Med* 213: 251-271
632 Lin CC, Bradstreet TR, Schwarzkopf EA, Sim J, Carrero JA, Chou C, Cook LE, Egawa T, Taneja R,
633 Murphy TL *et al* (2014) Bhlhe40 controls cytokine production by T cells and is essential for
634 pathogenicity in autoimmune neuroinflammation. *Nat Commun* 5: 3551
635 Martinez-Llordella M, Esensten JH, Bailey-Bucktrout SL, Lipsky RH, Marini A, Chen J, Mughal M,
636 Mattson MP, Taub DD, Bluestone JA (2013) CD28-inducible transcription factor DEC1 is required
637 for efficient autoreactive CD4+ T cell response. *J Exp Med* 210: 1603-1619
638 Miller CH, Klawon DEJ, Zeng S, Lee V, Socci ND, Savage PA (2020) Eomes identifies thymic
639 precursors of self-specific memory-phenotype CD8(+) T cells. *Nat Immunol* 21: 567-577

640 Nenna R, Papoff P, Moretti C, Pierangeli A, Sabatino G, Costantino F, Soscia F, Cangiano G, Ferro
641 V, Mennini M *et al* (2011) Detection of respiratory viruses in the 2009 winter season in Rome:
642 2009 influenza A (H1N1) complications in children and concomitant type 1 diabetes onset. *Int J*
643 *Immunopathol Pharmacol* 24: 651-659
644 Pacheco Y, Acosta-Ampudia Y, Monsalve DM, Chang C, Gershwin ME, Anaya JM (2019) Bystander
645 activation and autoimmunity. *J Autoimmun* 103: 102301
646 Pane JA, Coulson BS (2015) Lessons from the mouse: potential contribution of bystander
647 lymphocyte activation by viruses to human type 1 diabetes. *Diabetologia* 58: 1149-1159
648 Pane JA, Webster NL, Coulson BS (2014) Rotavirus activates lymphocytes from non-obese diabetic
649 mice by triggering toll-like receptor 7 signaling and interferon production in plasmacytoid
650 dendritic cells. *PLoS Pathog* 10: e1003998
651 Park JE, Botting RA, Dominguez Conde C, Popescu DM, Lavaert M, Kunz DJ, Goh I, Stephenson E,
652 Ragazzini R, Tuck E *et al* (2020) A cell atlas of human thymic development defines T cell repertoire
653 formation. *Science* 367
654 Pellicci DG, Koay HF, Berzins SP (2020) Thymic development of unconventional T cells: how NKT
655 cells, MAIT cells and gammadelta T cells emerge. *Nat Rev Immunol* 20: 756-770
656 Piper C, Zhou V, Komorowski R, Szabo A, Vincent B, Serody J, Alegre ML, Edelson BT, Taneja R,
657 Drobyski WR (2020) Pathogenic Bhlhe40+ GM-CSF+ CD4+ T cells promote indirect alloantigen
658 presentation in the GI tract during GVHD. *Blood* 135: 568-581
659 Savage AK, Constantinides MG, Han J, Picard D, Martin E, Li B, Lantz O, Bendelac A (2008) The
660 transcription factor PLZF directs the effector program of the NKT cell lineage. *Immunity* 29: 391-
661 403
662 Scotet E, Peyrat MA, Saulquin X, Retiere C, Couedel C, Davodeau F, Dulphy N, Toubert A, Bignon
663 JD, Lim A *et al* (1999) Frequent enrichment for CD8 T cells reactive against common herpes viruses
664 in chronic inflammatory lesions: towards a reassessment of the physiopathological significance of
665 T cell clonal expansions found in autoimmune inflammatory processes. *Eur J Immunol* 29: 973-
666 985
667 Seddon B, Legname G, Tomlinson P, Zamoyska R (2000) Long-term survival but impaired
668 homeostatic proliferation of Naive T cells in the absence of p56lck. *Science* 290: 127-131
669 Serra P, Santamaria P (2019) Antigen-specific therapeutic approaches for autoimmunity. *Nat*
670 *Biotechnol* 37: 238-251
671 Sosinowski T, White JT, Cross EW, Haluszczak C, Marrack P, Gapin L, Kedl RM (2013) CD8alpha+
672 dendritic cell trans presentation of IL-15 to naive CD8+ T cells produces antigen-inexperienced T
673 cells in the periphery with memory phenotype and function. *J Immunol* 190: 1936-1947
674 Stromnes IM, Goverman JM (2006) Active induction of experimental allergic encephalomyelitis.
675 *Nat Protoc* 1: 1810-1819
676 Su LF, Davis MM (2013) Antiviral memory phenotype T cells in unexposed adults. *Immunol Rev*
677 255: 95-109

678 Su LF, Kidd BA, Han A, Kotzin JJ, Davis MM (2013) Virus-specific CD4(+) memory-phenotype T
679 cells are abundant in unexposed adults. *Immunity* 38: 373-383
680 Sutton CE, Lalor SJ, Sweeney CM, Brereton CF, Lavelle EC, Mills KH (2009) Interleukin-1 and IL-23
681 induce innate IL-17 production from gammadelta T cells, amplifying Th17 responses and
682 autoimmunity. *Immunity* 31: 331-341
683 Szabolcs P, Park KD, Reese M, Marti L, Broadwater G, Kurtzberg J (2003) Coexistent naive
684 phenotype and higher cycling rate of cord blood T cells as compared to adult peripheral blood.
685 *Exp Hematol* 31: 708-714
686 Tan LC, Mowat AG, Fazou C, Rostron T, Roskell H, Dunbar PR, Tournay C, Romagne F, Peyrat MA,
687 Houssaint E *et al* (2000) Specificity of T cells in synovial fluid: high frequencies of CD8(+) T cells
688 that are specific for certain viral epitopes. *Arthritis Res* 2: 154-164
689 Walker JA, Barlow JL, McKenzie AN (2013) Innate lymphoid cells--how did we miss them? *Nat Rev*
690 *Immunol* 13: 75-87
691 White JT, Cross EW, Burchill MA, Danhorn T, McCarter MD, Rosen HR, O'Connor B, Kedl RM (2016)
692 Virtual memory T cells develop and mediate bystander protective immunity in an IL-15-dependent
693 manner. *Nat Commun* 7: 11291
694 White JT, Cross EW, Kedl RM (2017) Antigen-inexperienced memory CD8(+) T cells: where they
695 come from and why we need them. *Nat Rev Immunol* 17: 391-400
696 Younes SA, Punkosdy G, Caucheteux S, Chen T, Grossman Z, Paul WE (2011) Memory phenotype
697 CD4 T cells undergoing rapid, nonburst-like, cytokine-driven proliferation can be distinguished
698 from antigen-experienced memory cells. *PLoS Biol* 9: e1001171
699 Yu F, Sharma S, Jankovic D, Gurram RK, Su P, Hu G, Li R, Rieder S, Zhao K, Sun B *et al* (2018) The
700 transcription factor Bhlhe40 is a switch of inflammatory versus antiinflammatory Th1 cell fate
701 determination. *J Exp Med* 215: 1813-1821

702

703 **Acknowledgements**

704 We thank Dr. Dongsoo Kyeong and Dr. Younhee Shin (Insilicogen Inc.) for supporting bioinformatic analysis
705 of the scRNA-seq data. We thank Mr. Yeon-Ho Kim and Ms. In Young Song for technical support in the FACS
706 sorting conducted at Hanyang LINC Analytical Equipment Center (Seoul) and the NIH tetramer core facility
707 (Emory University) for providing mouse CD1d PBS-57 (Biotinylated Monomer). We thank Prof. Jeehee Youn
708 (Hanyang University) for kindly providing CD45.1$^{+}$, Foxp3-GFP mice and Prof. Kwang Soon Kim (POSTECH)
709 for helping us purchase germ-free and antigen-free mice.

710 **Funding**

711 This research was supported by the Basic Science Research Program (NRF-2019R1A2C3006155) of the
712 National Research Foundation funded by the Korean government.

713 **Author contributions**

714 M.-Z.C., H.-G.L., and J.-M.C. conceptualized and designed this study. M.-Z.C., H.-G.L. performed and
715 analyzed most of the experiments including bioinformatic analysis. Y.J.L. supported conceptualization for
716 bioinformatic analyses. J.-W.Y., G.-R.K. and J.-H.K. supported experiments. R.T. and B.T.E. provided
717 Bhlhe40$^{-/-}$ and Bhlhe40$^{GFP}$. M.-Z.C., H.-G.L., and J.-M.C. wrote draft manuscript, and all authors reviewed the
718 manuscript. J.-M.C. supervised the analyses and acquired funding.

719 **Conflict of Interest**

720 The authors declare that they have no competing interests.

721 **Data and materials availability**

722 The data that support the findings of this study are available from the corresponding author upon reasonable
723 request. RNA-seq data have been deposited in the NCBI Gene Expression Omnibus.

724

725 **Figures**

726 **Figure 1. Single cell RNA-sequencing identifies distinct effector-like phenotypes in steady-state MP CD4$^+$**
727 **T cells.** (A) Representative flow cytometry plots showing the population of memory-phenotype (MP) CD4$^+$ T
728 cells (TCRβ$^+$CD1d tetramer$^-$CD8$^-$CD4$^+$CD25$^-$CD62L$^{low}$CD44$^{high}$) in murine spleens, thymuses, inguinal lymph
729 nodes (iLNs), lungs, mesenteric lymph nodes (mLNs), and Peyer's patches (PP). (B) tSNE plot of splenic MP
730 CD4$^+$ T cells isolated from 10-week-old specific-pathogen-free (SPF) mice. (C) Heatmap of differentially
731 expressed transcripts in splenic MP CD4$^+$ T cells. (D) Expression of selected genes used to define MP CD4$^+$ T
732 cell clusters. (E) Differential expression of transcription factors and chemokine receptors from splenic MP CD4$^+$
733 T cell clusters. (F) Flow cytometry plots of splenic MP CD4$^+$ T cells (TCRβ$^+$CD1d tetramer$^-$CD8$^-$CD4$^+$CD25$^-$
734 CD62L$^{low}$CD44$^{high}$) from SPF-, GF-, and AF-mice. (G) tSNE plot and (h) proportion of integrated splenic MP
735 CD4$^+$ T cells isolated from 10-week-old SPF- and GF-mice. (I) tSNE plot and (J) proportion of integrated mLN
736 MP CD4$^+$ T cells isolated from SPF- and GF-mice. (K) Pie chart representing the clonal size distribution of MP
737 CD4$^+$ T cells. (L) Diversity of the TCR repertoire in MP CD4$^+$ T cell subsets from SPF- and GF-mice.

738 **Figure 2. Phenotypic differences of MP CD4$^+$ T cells after exposure to IL-1 family and STAT activating**
739 **cytokines.** (A) Overview of experimental design. (B) UMAP representation of MP CD4$^+$ T cells stimulated
740 with IL-12 and/or IL-18 and IL-33 and/or IL-25 and IL-1β and/or IL-23 in the presence of IL-7. (C) Heatmap
741 and (D) violin plots of differentially expressed transcripts in cluster. (E) Individual cytokines conditions
742 visualized with UMAP. (F) MA plots of differentially expressed genes comparing IL-7 versus IL-12/18 or IL-
743 33/25 or IL-1β/23. (G) Heatmap representing gene expression of Resting-, Tfh-, Th1-, Th2-, Th17- and Treg-
744 related gene signatures in each cytokine condition. (H) Heatmap representing transcription activity. (I) Venn
745 diagram of transcriptional regulators predicted by the IPA. Numbers indicate the number of gene in each gate.
746 (J) MP CD4$^+$ T cells (TCRβ$^+$CD1d tetramer$^-$CD8$^-$CD4$^+$CD25$^-$CD62L$^{low}$CD44$^{high}$) were cultured for 5 days with

747 IL-12 and/or IL-18 and IL-33 and/or IL-25 and IL-1β and/or IL-23 in the presence of IL-7 or anti-CD3/anti-
748 CD28. Representative flow cytometry plots showing the expression of effector lineage markers in each cytokine
749 condition. (K) IFN-γ, TNF-α, IL-4, IL-5, IL-13, IL-17A, and GM-CSF were measured by ELISA (n=5). Data
750 are presented as the mean ± S.D. P values were calculated using Mann-Whitney U-test (*$p < 0.05$, **$p < 0.01$,
751 ***$p < 0.001$).

752 **Figure 3. Potential responder MP CD4$^+$ T cells express distinct chemokine receptors upon IL-12/IL-18**
753 **and IL-1β /IL-23 stimulation.** (A) tSNE plots and (B) proportion of MP CD4$^+$ T cells stimulated with IL-12
754 and IL-18 in the presence of IL-7 for 5 days. (C) Expression of selected Th1-related genes. (D) Selected
755 KEGG/GO terms in cluster 2,3,4 and 6 and (E) Ingenuity pathway analysis (IPA) in cluster 3,4 and 6 of IL-12-
756 and IL-18-responded MP CD4$^+$ T cells. (F) Pseudo-time trajectory: each cell is colored by its pseudo-time value
757 and (G) the expression level of the related genes. (H) tSNE plots and (I) proportion of MP CD4$^+$ T cells
758 stimulated with IL-1β and IL-23 in the presence of IL-7 for 5 days. (J) Expression of selected Th17-related
759 genes. (K) Selected KEGG/GO terms and (L) IPA of IL-1β- and IL-23-stimulated MP CD4$^+$ T cells (clusters 3,
760 4, 6). (M) Pseudo-times trajectory: each cell is colored by its pseudo-time value and (N) the transcription factor
761 activity and (O) expression level of the related genes.

762 **Figure 4. CCR6$^{high}$ MP CD4$^+$ T cells are bystander-activated by IL-1β and IL-23 to become pathogenic**
763 **Th17-like cells.** (A) Gating strategy of CCR6$^{high}$ and CCR6$^{low}$ MP CD4$^+$ T cells from SPF mice. (B) The
764 percentage of CCR6 expression in steady-state splenic MP CD4$^+$ T cells (n=6). (C) The expression of CCR6 in
765 SPF- vs. GF-MP CD4$^+$ T cells (n=4). (dD) Transcription factor expression level of T-bet and RORγt in FACS-
766 sorted CCR6$^{high}$ and CCR6$^{low}$ MP CD4$^+$ T cells and (E) the proportion (n=4). (F) Representative flow cytometry
767 plots showing the cytokine expression and (G) the average proportion of CCR6$^{high}$ MP CD4$^+$ T cells vs. CCR6$^{low}$
768 MP CD4$^+$ T cells (n = 6). CCR6$^{high}$ and CCR6$^{low}$ MP CD4$^+$ T cells were stimulated with IL-1β and/or IL-23 in
769 the presence of IL-7 for 5 days. (H) The representative proportion and (I) the average value showing the cytokine
770 producing cells (n=5). (J) Concentration of IL-17A, GM-CSF, and IFN-γ were analyzed by ELISA (n = 5). (K)
771 The proportion of RORγt$^+$ and Ki67$^+$ cells in CCR6$^{high}$ and CCR6$^{low}$ MP CD4$^+$ T cells. (L) Heatmap of selected
772 genes (M) Gene set enrichment analysis (GSEA) pathway enrichment plot related to "Cell Proliferation" and
773 "Pathogenic $T_H17$ signature" by bulk RNA-seq analysis. *q*, false discovery rate; NES, normalized enrichment
774 score. Data are presented as the mean ± S.D. All data of p values were calculated using Mann-Whitney U-test
775 (ND, not detected; NS, not significant; *$p < 0.05$, **$p < 0.01$, ***$p < 0.001$).

776 **Figure 5. CCR6$^{high}$ MP CD4$^+$ T cells are encephalitogenic and exacerbate autoimmune**
777 **neuroinflammation.** (A) Naïve CD4$^+$ T cells ($5 \times 10^4$) from 2D2 transgenic mice were adoptively transferred,
778 with or without CCR6$^{high}$ or CCR6$^{low}$ MP CD4$^+$ T cells ($1 \times 10^5$ CD45.1$^+$TCRβ$^+$CD1d tetramer$^-$CD4$^+$CD25$^-$
779 CD62L$^{low}$CD44$^{high}$), into Rag$^{-/-}$ mice who were immunized with $MOG_{35-55}$ in CFA. EAE clinical score was
780 monitored daily (n=15). (B) Absolute cell numbers of infiltrated CD45.1$^+$MP CD4$^+$ T cells in the spinal cord
781 and brain (n=8). (C) The representative plots and (D) absolute cell number of IL-17A, GM-CSF, and IFN-γ
782 producing cells were determined in MP CD4$^+$ T cells from the spinal cords and brains on days 12–13 after
783 immunization (n=8). (E) The representative dot plots and (F) the average value showing the percentage of 2D2

784 TCR ($V_\alpha3.2^+$ and $V_\beta11^+$) in spleens from 2D2 transgenic mice and C57BL/6 wild type mice (n=4). (G) FACS-
785 sorted 2D2 naïve $CD4^+$ T cells and MP $CD4^+$ T cells were cultured with $CD11c^+$ dendritic cells (MHC-
786 $II^+CD11c^+$) with or without $MOG_{35-55}$ peptide (50 μg/ml) for 3 days. CFSE levels were measured by flow
787 cytometry. Data are presented as the mean ± S.E.M in A and the mean ± S.D in B,D,F. *P* values were calculated
788 using two-way ANOVA or Mann-Whitney U-test (NS, not significant; *p < 0.05, **p < 0.01, ***p < 0.001).

789 **Figure 6. Bhlhe40 confers pathogenic functions of bystander $CCR6^{high}$ MP $CD4^+$ T cells by IL-1 and IL-**
790 **23.** (A) Predicted upstream network on IL-1β and IL-23 responded MP $CD4^+$ T cells by IPA. (B) The
791 representative histogram and average value showing the percentage of Bhlhe40 level in $CCR6^{high}$ and $CCR6^{low}$
792 MP $CD4^+$ T cells induced by IL-1β/IL-23 stimulation without TCR engagement (n=3). (C) The representative
793 percentage of IL-17A and GM-CSF expression compared to $Bhlhe40^{GFP}$ positive and negative cells in $CCR6^{high}$
794 MP $CD4^+$ T cells induced by IL-1β /IL-23 without TCR engagement for 5 days (n=3). (D) Representative flow
795 cytometry plots showing the cytokine expression and (E) average proportion of WT $CCR6^{high}$ MP $CD4^+$ T cells
796 vs. $Bhlhe40^{-/-}$ $CCR6^{high}$ MP $CD4^+$ T cells (n = 3). (F) Naïve $CD4^+$ T cells ($5 \times 10^4$) from 2D2 transgenic mice
797 were adoptively transferred, with or without WT $CCR6^{high}$ or $Bhlhe40^{-/-}$ $CCR6^{high}$ MP $CD4^+$ T cells ($1 \times 10^5$,
798 $TCR\beta^+CD1d\ tetramer^-CD4^+CD25^-CD62L^{low}CD44^{high}$), into $Rag^{-/-}$ mice who were immunized with $MOG_{35-55}$ in
799 CFA. EAE clinical score was monitored daily (n=5). (G) Representative flow cytometry plots and (H) absolute
800 cell numbers of infiltrated 2D2 TCR $(V_\beta11^+)^-$ MP $CD4^+$ T cells (gating from $CD45^+CD4^+$) and IL-17A, GM-
801 CSF, and IFN-γ producing cells from the spinal cords and brain on days 13 after immunization (n=5). (I) Naïve
802 $CD4^+$ T cells ($5 \times 10^4$) from 2D2 transgenic mice were adoptively transferred, with or without WT $CCR6^{high}$ or
803 WT $CCR6^{low}$ or $GM\text{-}CSF^{-/-}$ $CCR6^{high}$ or $GM\text{-}CSF^{-/-}$ $CCR6^{low}$ MP $CD4^+$ T cells ($1 \times 10^5$, $CD45.1^+TCR\beta^+CD1d$
804 $tetramer^-CD4^+CD25^-CD62L^{low}CD44^{high}$), into $Rag^{-/-}$ mice who were immunized with $MOG_{35-55}$ in CFA. EAE
805 clinical score was monitored daily (n=9). Data are presented as the mean ± S.E.M in f,i and the mean ± S.D in
806 b,c,d,e,g,h values were calculated using two-way ANOVA or Mann-Whitney U-test (NS, not significant; *p <
807 0.05, **p < 0.01, ***p < 0.001).

808

**Figure 1.**

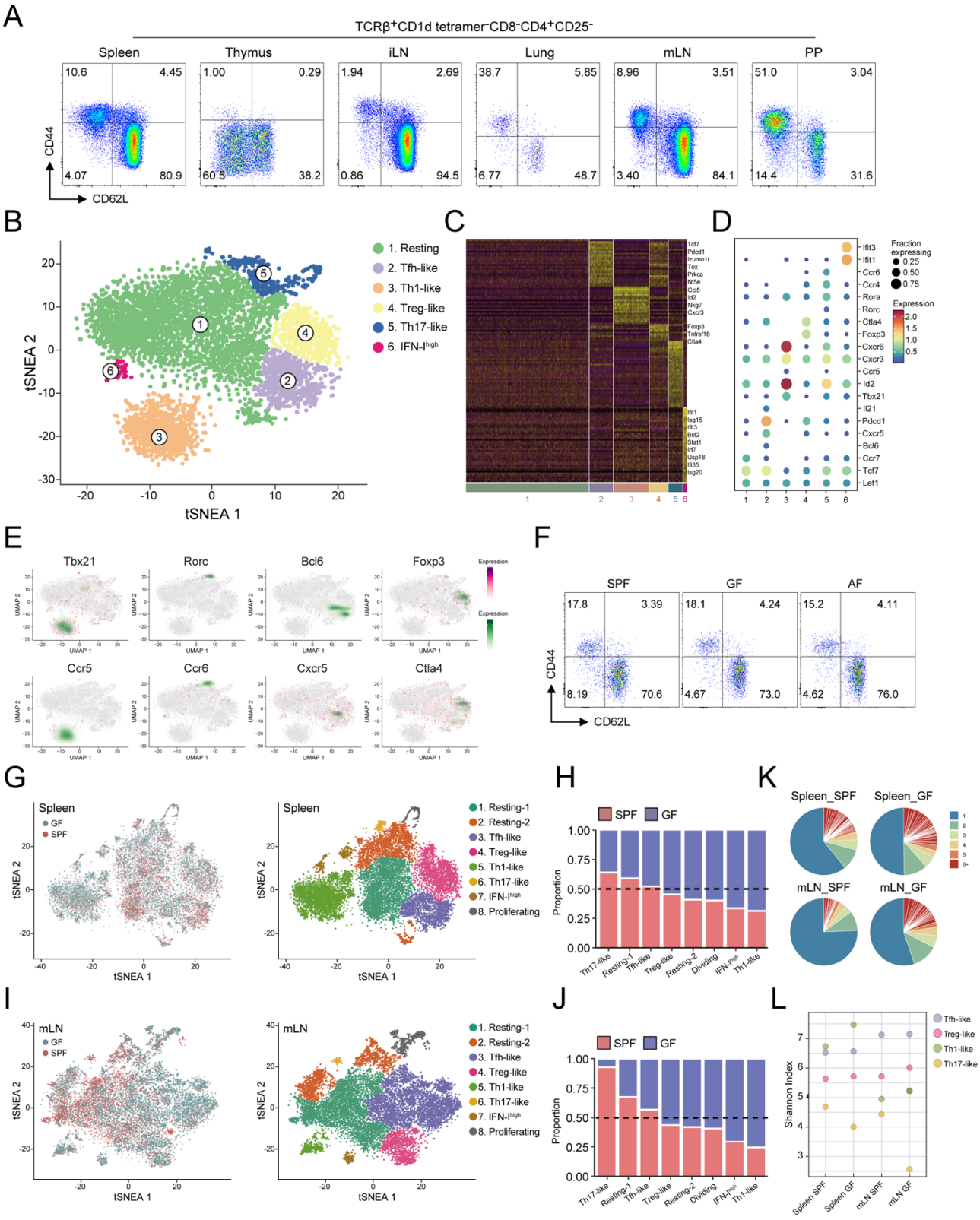


809

810

**Figure 2.**

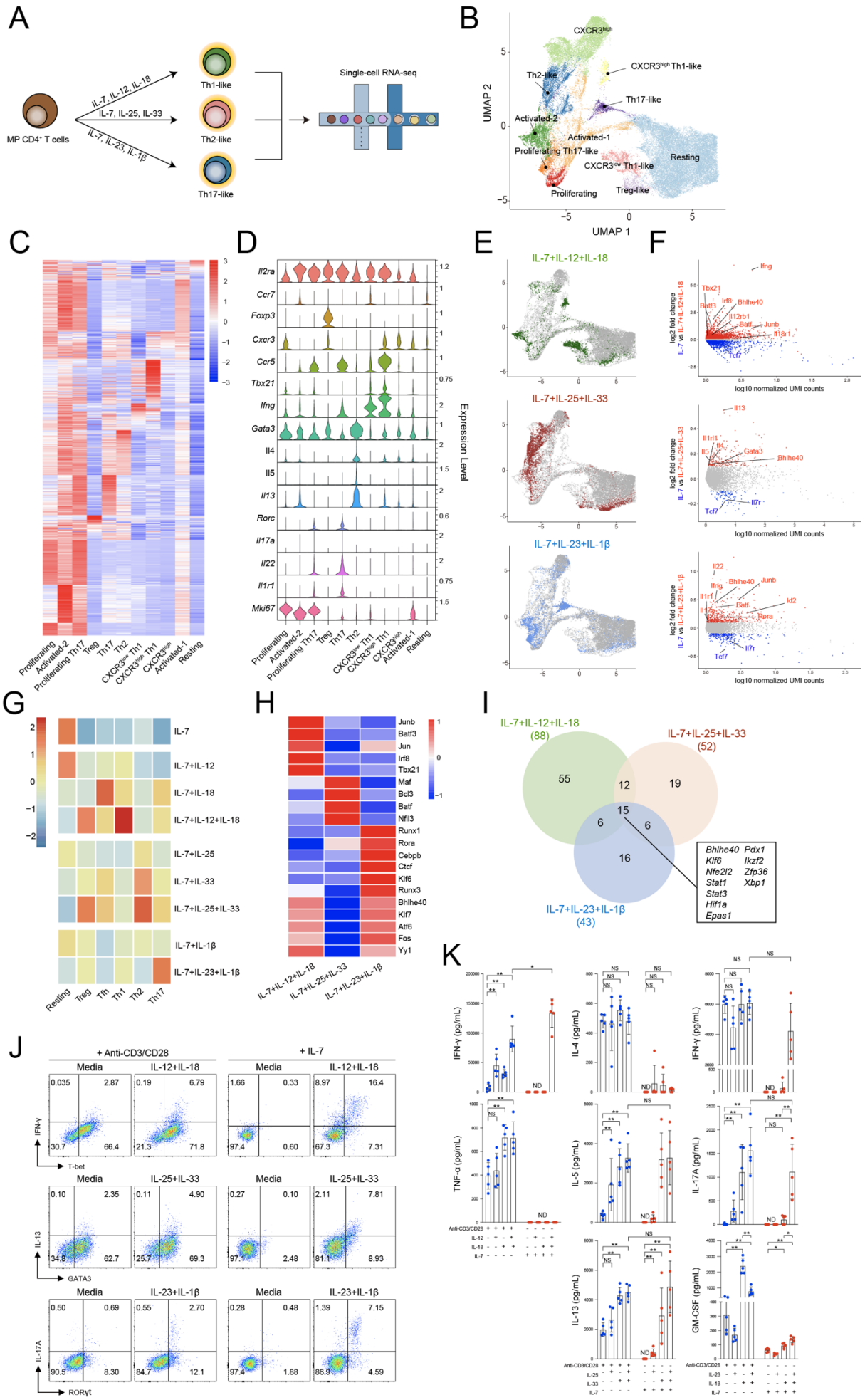
A
MP CD4+ T cells
IL-7, IL-12, IL-18
IL-7, IL-25, IL-33
IL-7, IL-23, IL-1β
Th1-like
Th2-like
Th17-like
Single-cell RNA-seq
B
UMAP 1
UMAP 2
CXCR3high
CXCR3high Th1-like
Th2-like
Th17-like
Activated-2
Activated-1
Proliferating Th17-like
CXCR3low Th1-like
Resting
Proliferating
Treg-like
C
D
Expression Level
Proliferating
Activated-2
Proliferating Th17
Treg
Th17
Th2
CXCR3low Th1
CXCR3high Th1
CXCR3high
Activated-1
Resting
E
IL-7+IL-12+IL-18
IL-7+IL-25+IL-33
IL-7+IL-23+IL-1β
F
log2 fold change
log10 normalized UMI counts
G
IL-7
IL-7+IL-12
IL-7+IL-18
IL-7+IL-12+IL-18
IL-7+IL-25
IL-7+IL-33
IL-7+IL-25+IL-33
IL-7+IL-1β
IL-7+IL-23+IL-1β
Resting
Treg
Tfh
Th1
Th2
Th17
H
IL-7+IL-12+IL-18
IL-7+IL-25+IL-33
IL-7+IL-23+IL-1β
I
IL-7+IL-12+IL-18 (88)
IL-7+IL-25+IL-33 (52)
IL-7+IL-23+IL-1β (43)
Bhlhe40 Pdx1
Klf6 Ikzf2
Nfe2l2 Zfp36
Stat1 Xbp1
Stat3
Hif1a
Epas1
J
+ Anti-CD3/CD28
+ IL-7
Media
IL-12+IL-18
IL-25+IL-33
IL-23+IL-1β
IFN-γ
T-bet
IL-13
GATA3
IL-17A
RORγt
K
IFN-γ (pg/mL)
IL-4 (pg/mL)
TNF-α (pg/mL)
IL-5 (pg/mL)
IL-17A (pg/mL)
IL-13 (pg/mL)
GM-CSF (pg/mL)
ND
NS

811

# Figure 3.

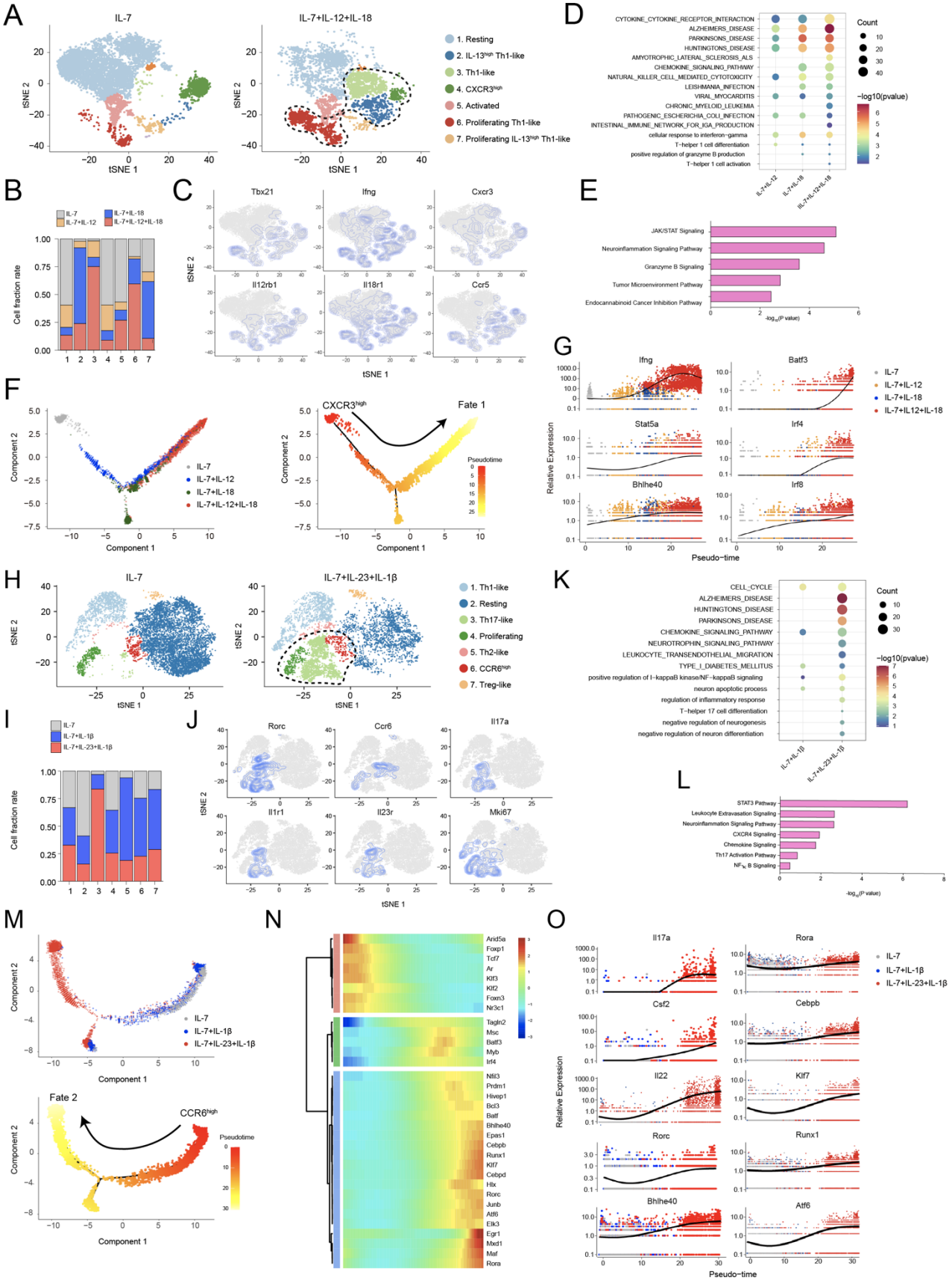
A
IL-7
IL-7+IL-12+IL-18
tSNE 1
tSNE 2
1. Resting
2. IL-13high Th1-like
3. Th1-like
4. CXCR3high
5. Activated
6. Proliferating Th1-like
7. Proliferating IL-13high Th1-like
B
Cell fraction rate
C
Tbx21
Ifng
Cxcr3
Il12rb1
Il18r1
Ccr5
D
CYTOKINE_CYTOKINE_RECEPTOR_INTERACTION
ALZHEIMERS_DISEASE
PARKINSONS_DISEASE
HUNTINGTONS_DISEASE
AMYOTROPHIC_LATERAL_SCLEROSIS_ALS
CHEMOKINE_SIGNALING_PATHWAY
NATURAL_KILLER_CELL_MEDIATED_CYTOTOXICITY
LEISHMANIA_INFECTION
VIRAL_MYOCARDITIS
CHRONIC_MYELOID_LEUKEMIA
PATHOGENIC_ESCHERICHIA_COLI_INFECTION
INTESTINAL_IMMUNE_NETWORK_FOR_IGA_PRODUCTION
cellular response to interferon−gamma
T−helper 1 cell differentiation
positive regulation of granzyme B production
T−helper 1 cell activation
Count
−log10(pvalue)
E
JAK/STAT Signaling
Neuroinflammation Signaling Pathway
Granzyme B Signaling
Tumor Microenvironment Pathway
Endocannabinoid Cancer Inhibition Pathway
F
Component 1
Component 2
CXCR3high
Fate 1
Pseudotime
G
Ifng
Batf3
Stat5a
Irf4
Bhlhe40
Irf8
Relative Expression
Pseudo−time
H
IL-7
IL-7+IL-23+IL-1β
1. Th1-like
2. Resting
3. Th17-like
4. Proliferating
5. Th2-like
6. CCR6high
7. Treg-like
I
Cell fraction rate
J
Rorc
Ccr6
Il17a
Il1r1
Il23r
Mki67
K
CELL_CYCLE
ALZHEIMERS_DISEASE
HUNTINGTONS_DISEASE
PARKINSONS_DISEASE
CHEMOKINE_SIGNALING_PATHWAY
NEUROTROPHIN_SIGNALING_PATHWAY
LEUKOCYTE_TRANSENDOTHELIAL_MIGRATION
TYPE_I_DIABETES_MELLITUS
positive regulation of I−kappaB kinase/NF−kappaB signaling
neuron apoptotic process
regulation of inflammatory response
T−helper 17 cell differentiation
negative regulation of neurogenesis
negative regulation of neuron differentiation
L
STAT3 Pathway
Leukocyte Extravasation Signaling
Neuroinflammation Signaling Pathway
CXCR4 Signaling
Chemokine Signaling
Th17 Activation Pathway
NF-κB Signaling
M
Fate 2
CCR6high
N
Arid5a
Foxp1
Tcf7
Ar
Klf3
Klf2
Foxn3
Nr3c1
Tagln2
Msc
Batf3
Myb
Irf4
Ntf3
Prdm1
Hivep1
Bcl3
Batf
Bhlhe40
Epas1
Cebpb
Runx1
Klf7
Cebpd
Hbx
Rorc
Junb
Atf6
Elk3
Egr1
Mxd1
Maf
Rora
O
Il17a
Rora
Csf2
Cebpb
Il22
Klf7
Rorc
Runx1
Bhlhe40
Atf6
Relative Expression
Pseudo−time

814

# Figure 4.

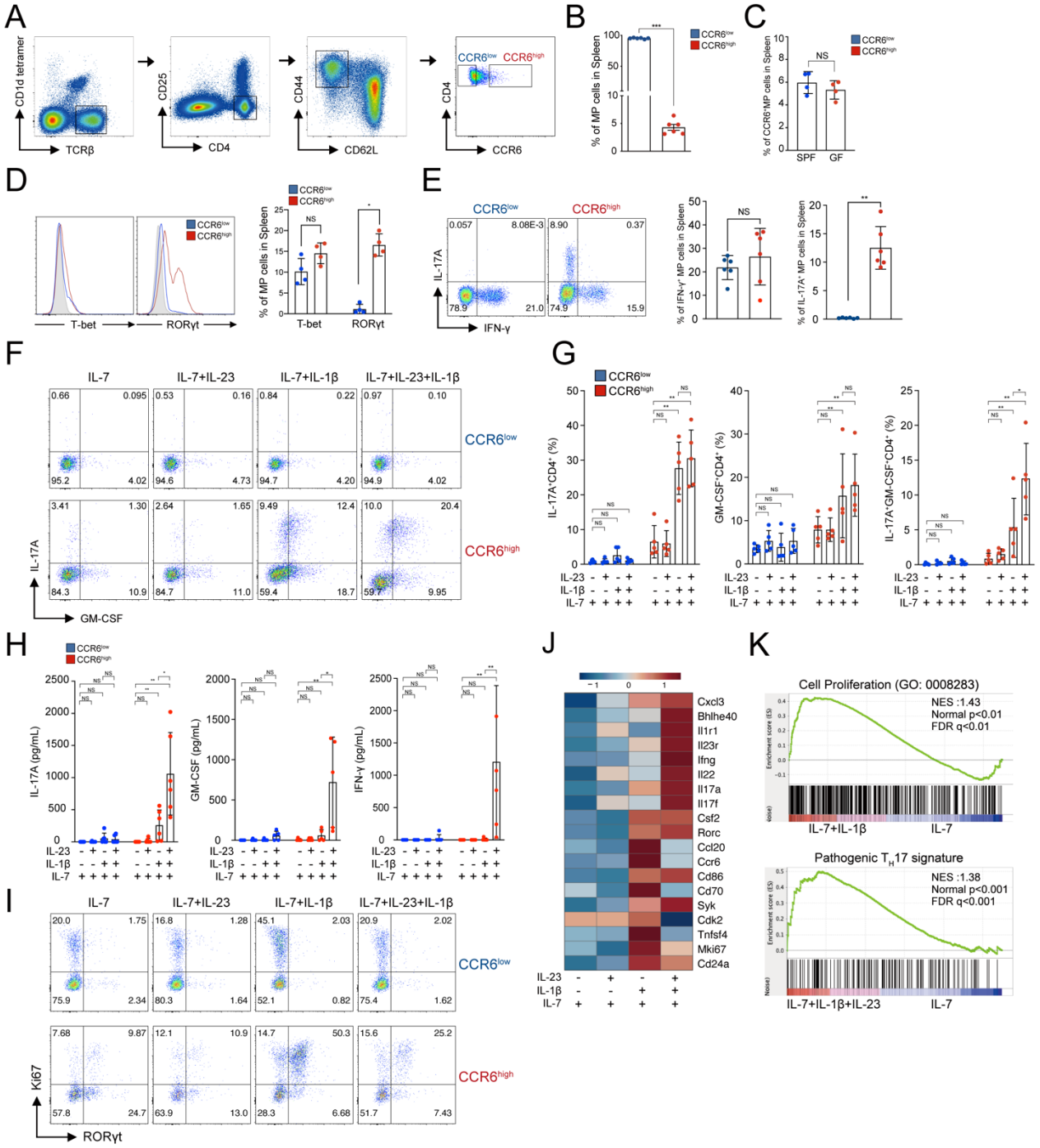


815

# Figure 5.

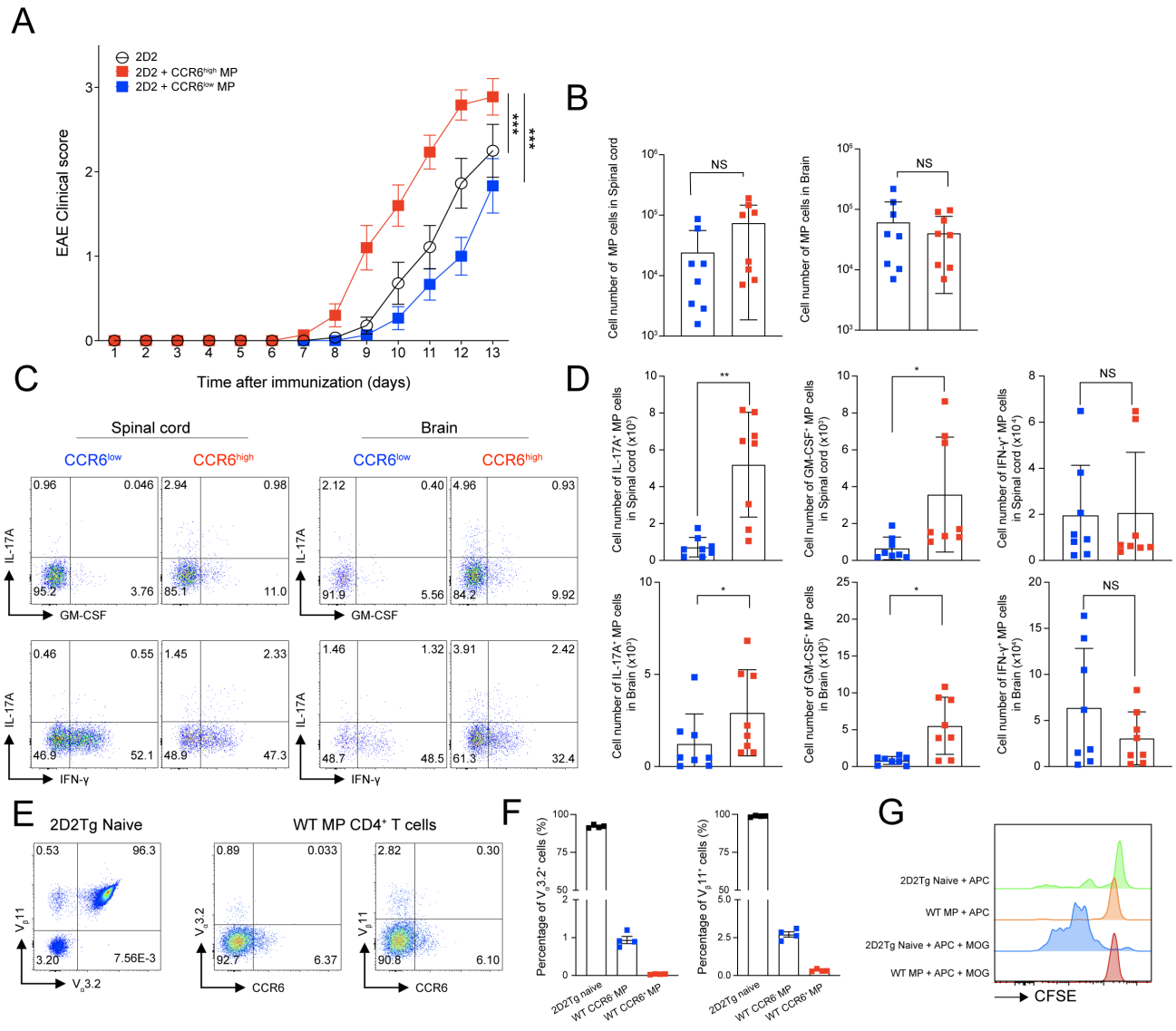
A
2D2
2D2 + CCR6high MP
2D2 + CCR6low MP
EAE Clinical score
Time after immunization (days)
***
***
B
Cell number of MP cells in Spinal cord
Cell number of MP cells in Brain
NS
NS
C
Spinal cord
Brain
CCR6low
CCR6high
IL-17A
GM-CSF
IFN-γ
D
Cell number of IL-17A+ MP cells in Spinal cord (x10³)
Cell number of GM-CSF+ MP cells in Spinal cord (x10³)
Cell number of IFN-γ+ MP cells in Spinal cord (x10³)
Cell number of IL-17A+ MP cells in Brain (x10³)
Cell number of GM-CSF+ MP cells in Brain (x10³)
Cell number of IFN-γ+ MP cells in Brain (x10³)
NS
E
2D2Tg Naive
WT MP CD4+ T cells
Vβ11
Vα3.2
CCR6
F
Percentage of Vα3.2+ cells (%)
Percentage of Vβ11+ cells (%)
2D2Tg naive
WT CCR6- MP
WT CCR6+ MP
G
2D2Tg Naive + APC
WT MP + APC
2D2Tg Naive + APC + MOG
WT MP + APC + MOG
CFSE

# Figure 6.

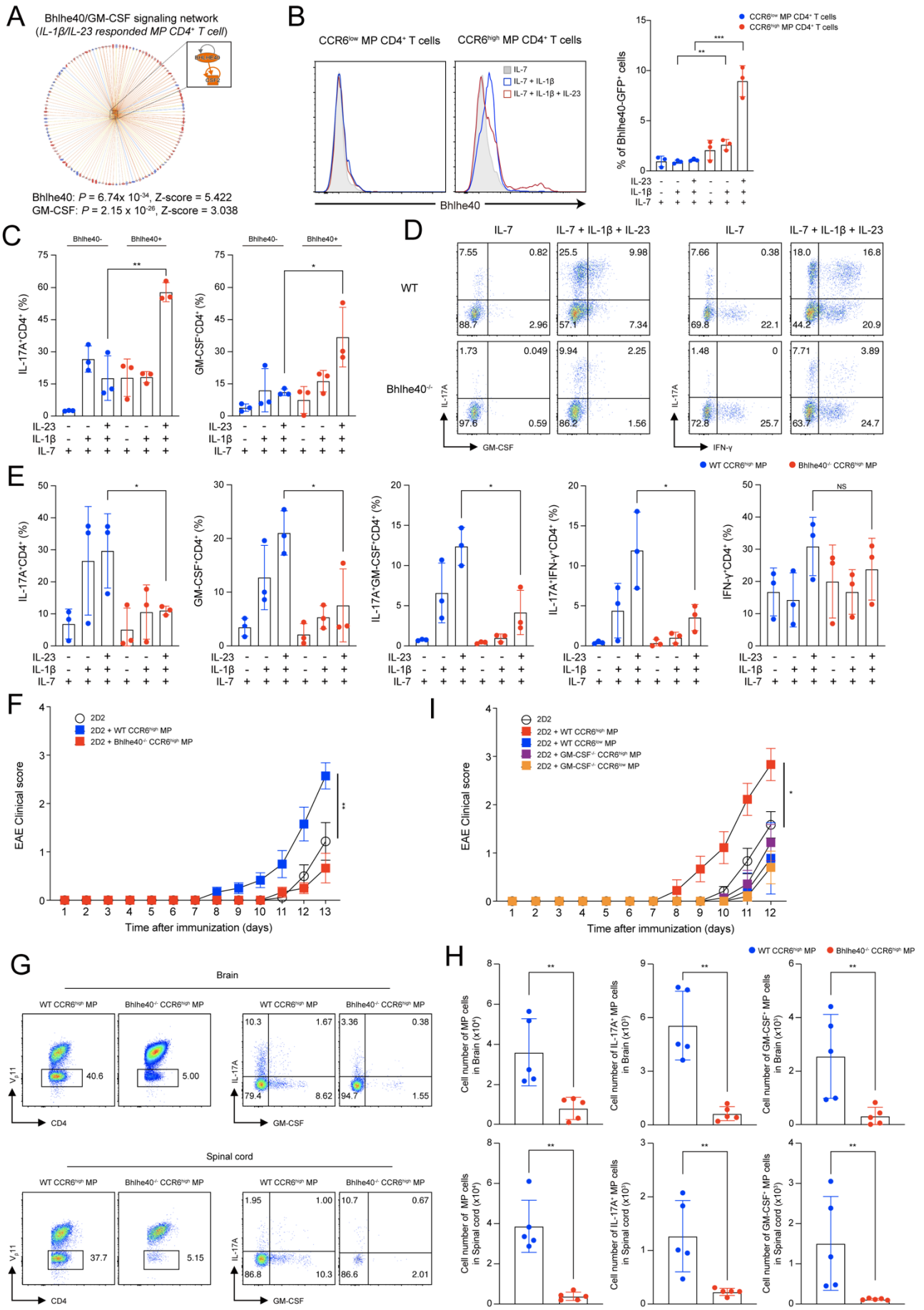


819

820

# Supporting Information

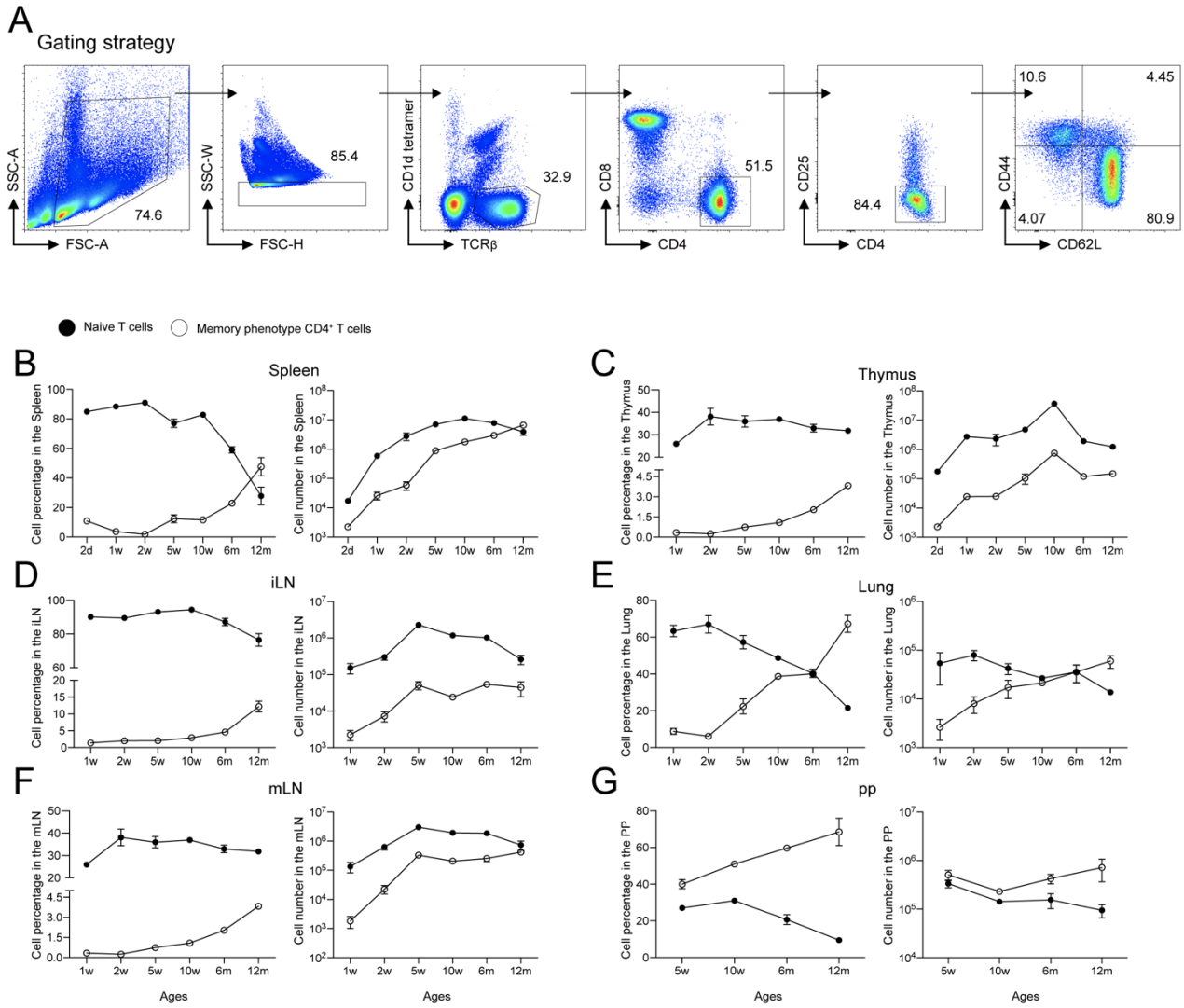


**Figure S1. CD44$^{high}$ memory phenotype (MP) CD4$^{+}$ T cells increase with age in mice.** (A) Gating strategy of Splenic MP CD4$^{+}$ T cells (TCRβ$^{+}$CD1d tetramer$^{-}$CD8$^{-}$CD4$^{+}$CD25$^{-}$CD62L$^{low}$CD44$^{high}$). Analysis of cell percentage and number of naïve (TCRβ$^{+}$CD1d tetramer$^{-}$CD8$^{-}$CD4$^{+}$CD25$^{-}$CD62L$^{high}$CD44$^{low}$) and MP CD4$^{+}$ T cells (TCRβ$^{+}$CD1d tetramer$^{-}$CD8$^{-}$CD4$^{+}$CD25$^{-}$CD62L$^{low}$CD44$^{high}$) by age from (B) the spleen, (C) thymus, (D) iLN, (E) lung, (F) mLN, and (G) PP.

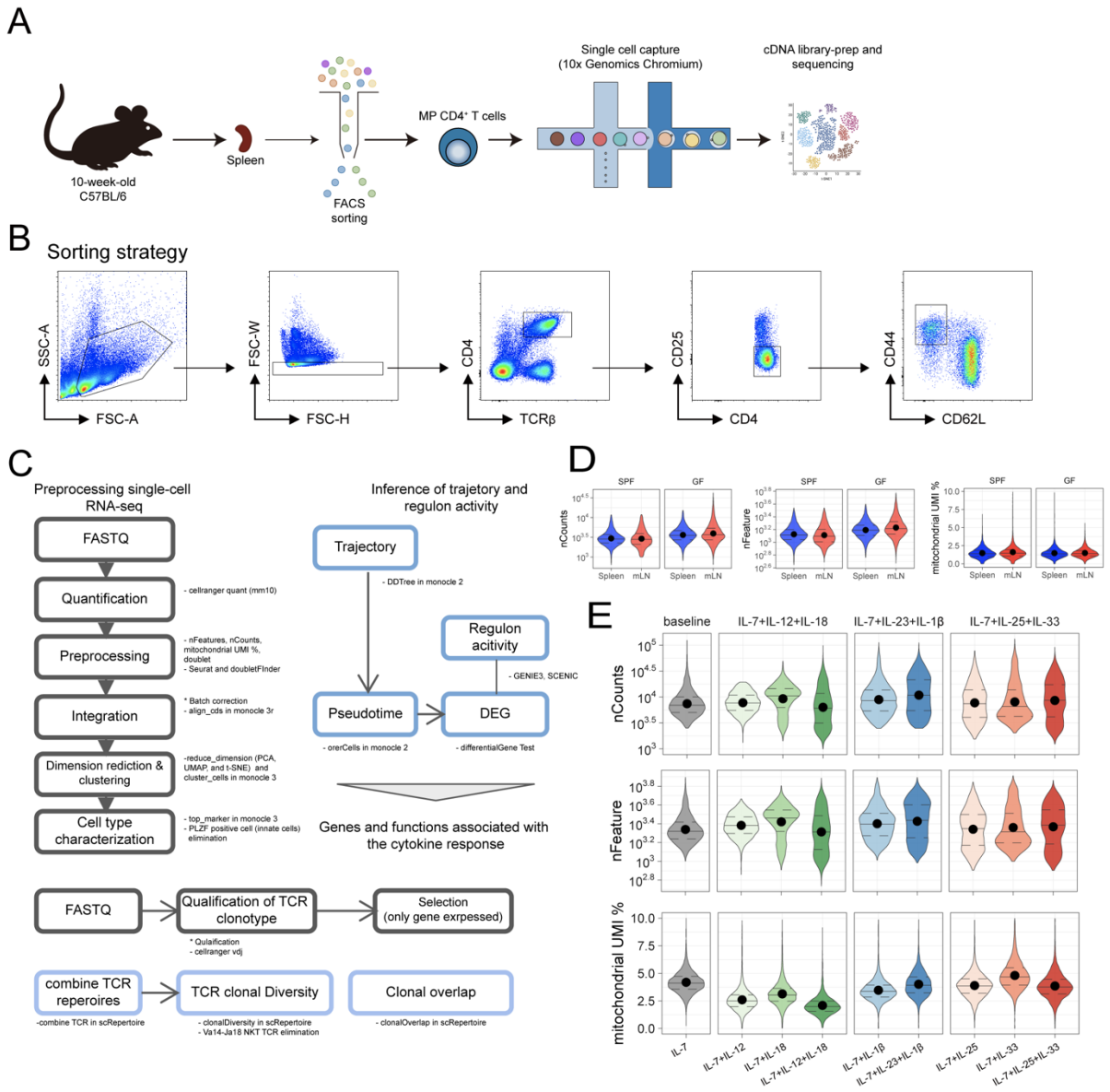


827

**Figure S2. Strategy and flow of single cell RNA-sequencing analysis.** (A) Visual concept of scRNA-seq for MP $CD4^+$ T cells. (B) Gating strategy of splenic MP ($TCR\beta^+CD4^+CD25^-CD62L^{low}CD44^{high}$) $CD4^+$ T cells. (C) Workflow of scRNA-seq and TCR-seq of PLZF and TCR $V_\alpha14$-$J_\alpha18$ (TRAV11-TRAJ18) negative MP $CD4^+$ T cells. (D) Quality measures of splenic and mLN MP $CD4^+$ T cells from SPF- and GF–housed mice. (E) QC metrics for each condition of MP $CD4^+$ T cells. (nFeature: the number of expressed genes per cell, nCounts: the number of total UMI counts per cell, mitochondrial UMI %: the percentage of UMI counts of mitochondrial genes per cell)

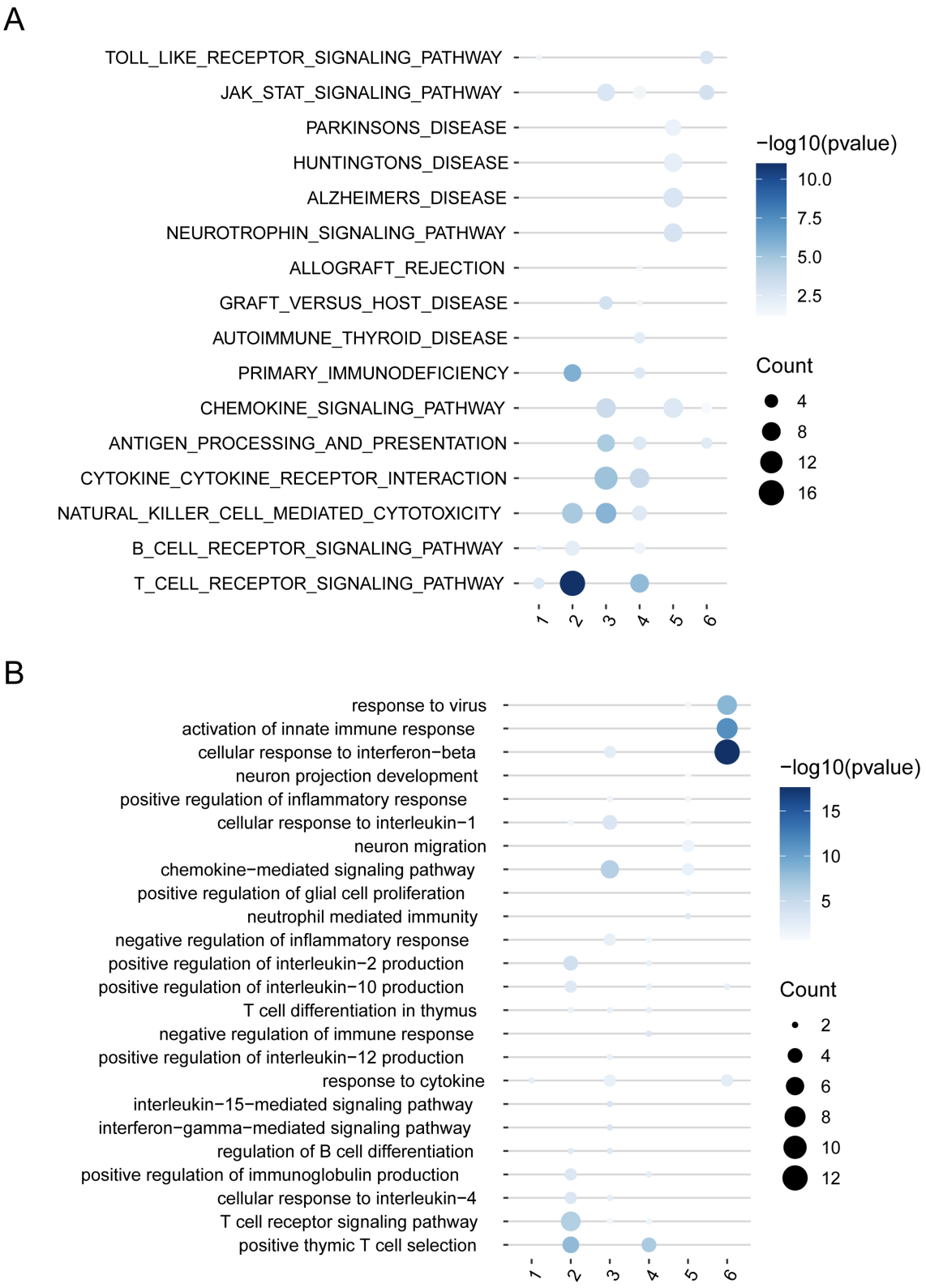


**Figure S3. KEGG/GO analysis of steady-state MP CD4$^{+}$ T cells.** Selected (A) KEGG and (B) GO terms in each subpopulation of splenic MP CD4$^{+}$ T cells.

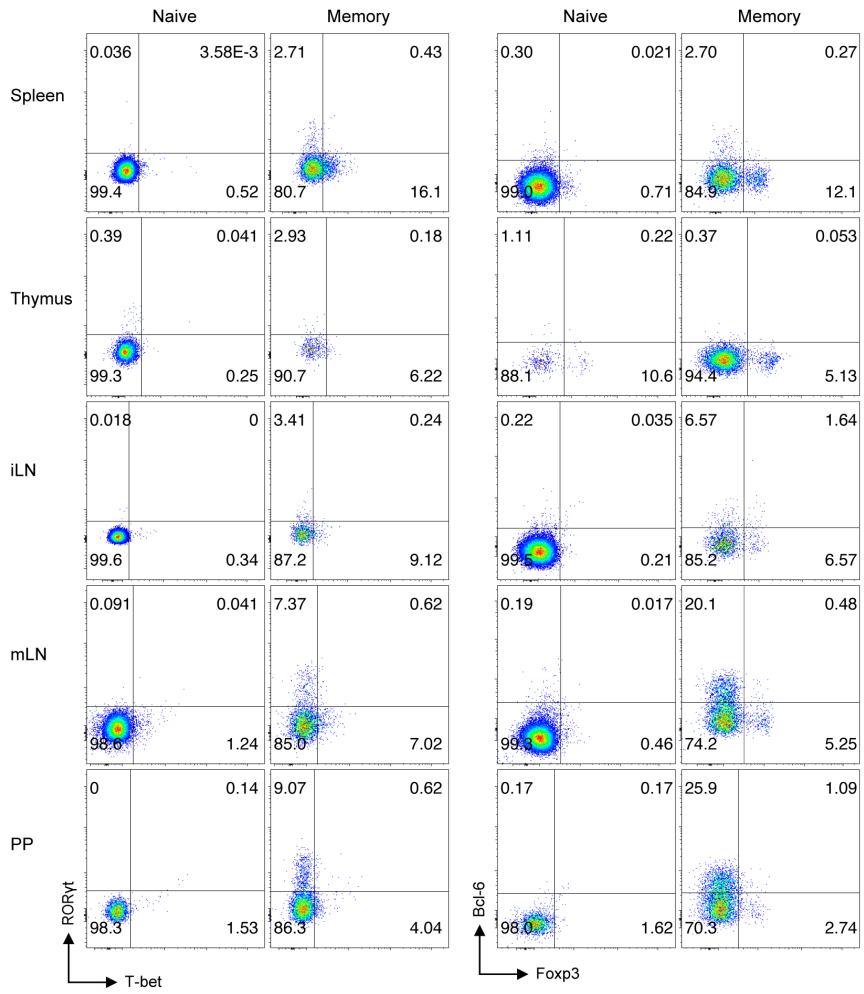


**Figure S4. Effector T cell lineage–specific marker expression in MP CD4$^+$ T cells.** Transcription factor expression levels of T-bet, RORγt, Bcl-6, and Foxp3 in naïve and MP CD4$^+$ T cells from the spleen, thymus, iLN, mLN, and PP.

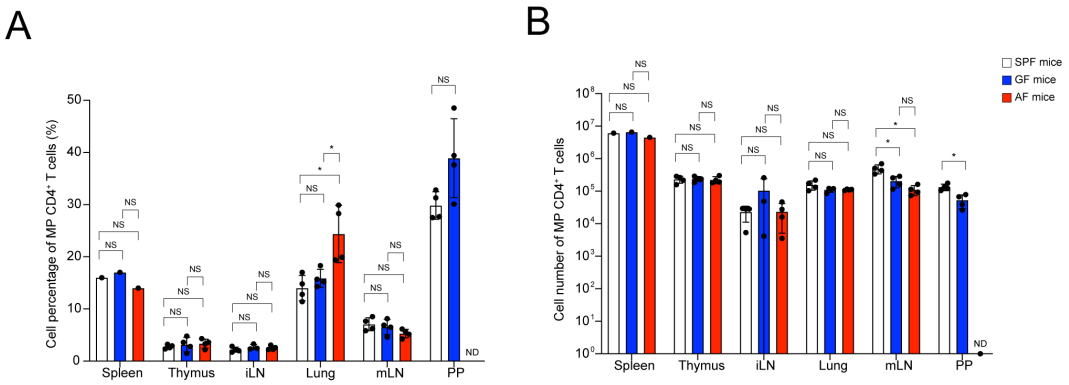


**Figure S5. Comparison of MP CD4$^+$ T cells in tissues from SPF, GF, and AF mice.** (A) Proportion and (B) number of MP CD4$^+$ T cells in the spleen, thymus, iLN, lung, mLN, and PP in SPF, GF, and AF mice (n=4). Data are presented as the mean ± S.D. P values were calculated using Mann-Whitney U-test (ND, not detected; NS, not significant; *$p < 0.05$, **$p < 0.01$, ***$p < 0.001$).

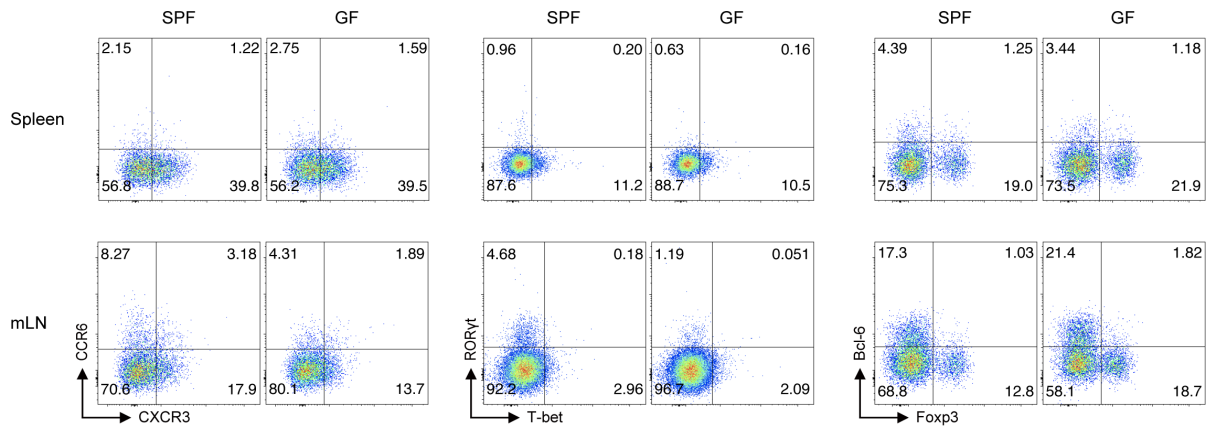


**Figure S6. Effector T cell lineage–specific chemokine receptors and transcription factors in MP CD4$^{+}$ T cells from SPF and GF mice.** Expression of chemokine receptor of CCR6, CXCR3 and transcription factors of T-bet, RORγt, Bcl-6, and Foxp3 in spleen- and mLN-derived MP CD4$^{+}$ T cells from SPF and GF mice.

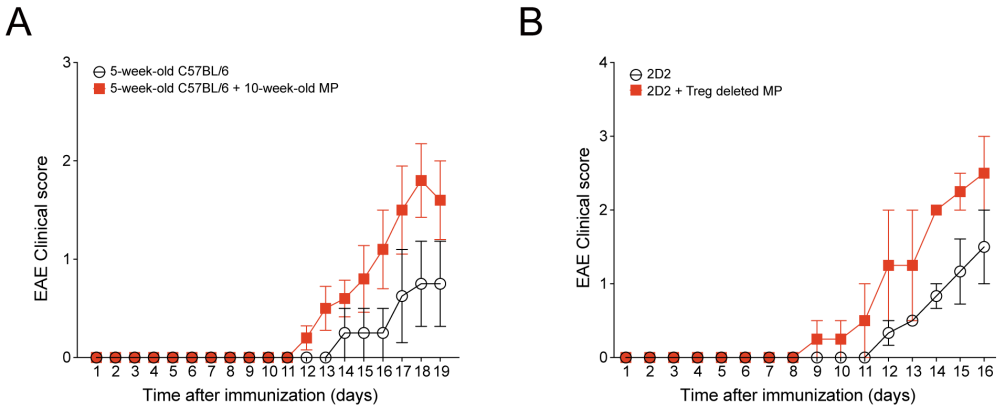


**Figure S7. MP CD4$^{+}$ T cells exacerbate autoimmune encephalomyelitis.** (A) 5-week-old C57BL/6 mice with or without adoptively transferred 5 × 10$^{5}$ MP CD4$^{+}$ T cells (TCRβ$^{+}$CD1d tetramer$^{-}$CD4$^{+}$Foxp3$^{-}$CD62L$^{low}$CD44$^{high}$) from 10-week-old Foxp3-GFP mice were induced EAE by MOG$_{35-55}$ in CFA (n=4). (B) 5 × 10$^{4}$ naïve CD4$^{+}$ T cells (TCRβ$^{+}$CD4$^{+}$V$_{\beta}$11$^{+}$CD25$^{-}$CD62L$^{high}$CD44$^{low}$) from 2D2 transgenic mice were adoptively transferred, with or without 5 ×10$^{5}$ splenic Treg-deleted MP CD4$^{+}$ T cells (TCRβ$^{+}$CD1d tetramer$^{-}$CD4$^{+}$Foxp3$^{-}$CD62L$^{low}$CD44$^{high}$) sorted from Foxp3-GFP mice, into Rag$^{-/-}$ mice who were immunized with MOG$_{35-55}$ in CFA (n = 3).